BAM
Bundesanstalt für Materialforschung und -prüfung

E.ON Energy Research Center | RWTH AACHEN UNIVERSITY

20th December 2023

Increasing energy efficiency and acceptance of heat pumps through realistic test procedures – Proof of concept on compensation method

Final report

Funded by
Deutsche Bundesstiftung Umwelt (DBU), Project reference 38677/01

Duration
23.01.2023-23.05.2023

Authors
Dr.-Ing. André Wachau
M.Sc. Daniel Mock
Federal Institute for Materials Research and Testing (BAM)
Section S.4 Ecodesign and Energy Labelling
andre.wachau@bam.de | Tel. +49 30 8104 4270

M.Sc. Stephan Göbel
Dr.-Ing. Christian Vering
Univ.-Prof. Dr.-Ing. Dirk Müller
RWTH Aachen University
E.ON Energy Research Center
Institute for Energy Efficient Buildings and Indoor Climate
stephan.goebel@eonerc.rwth-aachen.de | Tel. 0241 80 49772
CVering@eonerc.rwth-aachen.de | Tel. 0241 80 49786
DMueller@eonerc.rwth-aachen.de | Tel. 0241 80 49760

BAM
Bundesanstalt für Materialforschung und -prüfung

E.ON Energy Research Center | RWTH AACHEN UNIVERSITY

Content

List of figures

List of tables

Terms and symbols

Symbol and abbreviated terms	Denomination	Units
COP	Coefficient of Performance	-
DB	Dry bulb	-
WB	Wet bulb	-
$\dot{Q}_{\mathrm{designh}}$	Declared heating load at $T_{designh}$	kW
PRL_i	Part load ratio at test condition i	%
$P_h(T_j)$	Part-load capacity at temperature i	kW
$\dot{Q}_{\mathrm{HP}}$	Heating capacity	kW
P_{el}	Electrical power input	kW
T_{biv}	Bivalent temperature	°C
T_{designh}	Reference design temperature condition for heating	°C
TOL	Operation limit temperature	°C
$\vartheta_{i,A}$	Outdoor (ambient) temperature at test condition i	°C
$\vartheta_{\mathrm{B,set}}$	Indoor temperature set point of 20 °C	°C
ϑ_s	Indoor heat exchanger outlet water temperature (supply temperature)	°C
$\vartheta_{i,\mathrm{s,set}}$	Supply temperature set point at test condition i according to EN 14825:2022	°C
$\vartheta_{\mathrm{w,in}}$	Outdoor heat exchanger inlet water temperature (ground-source heat pumps)	°C
$\vartheta_{\mathrm{w,out}}$	Outdoor heat exchanger outlet water temperature (ground-source heat pumps)	°C
$\dot{m}_{\mathrm{W}}$	Mass flow in the heating circuit	kg/s
$\vartheta_{\mathrm{B,calc}}$	Calculated building temperature	°C
$\vartheta_{\mathrm{B,emu}}$	Emulated building temperature	°C
$\vartheta_{\mathrm{R,calc}}$	Calculated return temperature	°C
$\vartheta_{\mathrm{R,emu}}$	Emulated return temperature (indoor heat exchanger inlet water temperature)	°C
$\Delta\vartheta_{\mathrm{i,cond}}$	Temperature difference across the condenser	K
$\Delta\vartheta_{\mathrm{i,cond,design}}$	Design temperature difference across the condenser	K
$\dot{Q}_{\mathrm{HB}}$	Heat flux between mass H and mass B	kW
$\dot{Q}_{\mathrm{BA}}$	Heat flux between mass B and the ambient	kW
UA_{HB}	Thermal conductivity between mass H and B	J/K
UA_{BA}	Thermal conductivity between mass B and ambient	J/K
C_H	Thermal capacity of mass H	J/K
C_B	Thermal capacity of mass B	J/K
$\vartheta_{\mathrm{H,calc}}$	Calculated temperature of mass H	°C
Δt_{step}	Time step	s

1. Abstract

This project report presents results from a proof-of-concept (PoC) on a load-based performance test for hydronic heat pumps, namely the compensation method. The project partners have extended the compensation method developed by BAM by a simplified building model which is implemented in the test stand control to aligne inertia of different test stands. This yields more representative test results and higher reproducibility. To proof the feasibility and applicability of the new concept the interaction of the heat pump controller and test stand including the building model is studied. Three heat pumps from different manufacturers were tested in three different labs with different test stand architectures. Different control strategies of the heat pump were also tested (fixed vs. variable flow, additional indoor air temperature control). Moreover, a sensitivity analysis was performed to determine the impact of permissible deviations on the coefficient of performance. Thus, the project also aims to provide data to set permissible deviations in the BAM test guideline and identify aspects which must be improved. Finally, the impact of inertia on operating behaviour and COP is assessed to confirm the need for the building model integration.

The tests have shown that the building model can be implemented within few weeks in the most common test stand architectures (direct and indirect method) while achieving sufficient level of control on the return temperature. The tests under full and part-load conditions have proven realistic operating behaviour. An improvement potential of the test rig was identified to increase controllability during defrost which could be implemented successfully by the labs. It was also shown that the electrical back-up heater can be included in the test which yields more realistic test results. It could also be shown that inertia changes operating behaviour and should be aligned to ensure the same operation in all labs. It was found that the change in operating behaviour results in different COPs. Therefore, inertia of different labs must be aligned. The approach proposed by the project partners has been proven feasible and the results and findings from the proof of concept are transferred to standardisation at CEN/TC 113/WG 8 and to the review process of the Ecodesign and Energy Labelling regulations for space heaters on EU-level.

The successful proof of concept is followed by a validation phase to study reproducibility of the revised compensation method in a round robin test (38943/01). The round robin test will yield further data to improve the test guideline and allow participating labs to gain experience in load-based testing.

The round robin test and the proof of concept are funded by the Deutsche Bundesstiftung Umwelt (DBU). The Austrian Institute of Technology (AIT) and the Institut für Luft- und Kältetechnik gemeinnützige Gesellschaft mbH (ILK Dresden) were commissioned to perform the measurements within this project. The three tested heat pumps were kindly provided by different manufacturers.

This project report is published on the DBU-website.

2. Introduction

Heat pumps are a key technology for the heat transition in almost all sectors. Due to the adopted climate protection targets and the energy market situation that has been exacerbated by geopolitical events, ambitious expansion targets are being pursued at the level of the EU and its member states. Germany, in particular, is increasing the number of heat pumps installed from just under 200,000 in 2022 to 500,000 in 2024 and thus aims to install up to 6 million heat pumps by 2030. The installation and operation of heat pumps increase the demand for electricity, which must be covered by renewable energy sources in the future in order to achieve consistent decarbonisation. In order to keep both grid utilisation and the demand for renewable energy sources as low as possible, heat pumps must be installed in a high-quality manner and operated with maximum energy efficiency.

At the EU level, the Ecodesign Regulation EU 813/2013 sets minimum requirements for the energy efficiency of heat pumps for space heating, while the EU energy label (EU 811/2013) creates transparency for consumers and design incentives for manufacturers by rating appliances according to energy efficiency. The energy efficiency of heat pumps is measured according to the so-called harmonised standards EN 14511 and EN 14825, compliance with which triggers the presumption of conformity and is thus quasi-binding. The requirement level of the regulations is thus strongly influenced by the design of the test standards and the underlying measurement procedure. Therefore, generally accepted quality criteria are applied to the test procedures: (a) good repeatability and reproducibility, (b) representativeness, (c) fair comparison between different units, (d) cost and time expenditure, and (e) independency of testing (no intervention/assistance by the manufacturer in the test). However, the current test standards for heat pumps must be improved further concerning these criteria and adapted to the technical development of heat pumps (inverter technology). Based on older heat pumps with fixed speed compressors (on/off units) and for reproducibility reasons, the test is carried out under quasi-steady state conditions today with fixed compressor speed and inactive control of the heat pump. This means that the heating capacity of the units must be individually adjusted at partial load, and heat pumps are consequently measured and evaluated under non-uniform operating and test conditions. In addition, testing is only possible with the manufacturer's support, and independent testing by market surveillance authorities is thus essentially impossible. [1]

In principle, so-called load-based test methods (compensation method) can solve the problems above because the heat pump controller is active during the test, and the compressor speed is no longer fixed. The machines show realistic operating behaviour and go into cycle operation under part load conditions. The prescribed load conditions are actually achieved, and the comparability of heat pumps is ensured for planners, installers and consumers. In addition, no test mode and frequency data are necessary for the test, so testing can be carried out independently from manufacturer.

However, the introduction of load-based methods brings challenges concerning the reproducibility of the results since, in contrast to standard testing, which is carried out under stationary test conditions, the test bench's and the heat pump's controller also interact under dynamic operating conditions (cycle operation).

BAM has developed a load-based test method (compensation method) as part of a research project ("Support for market surveillance – NAPE" (2015-2022), measure of the "National Action Plan for Energy Efficiency" (NAPE) of the Federal government [2]), which tests heat pumps under normal operating conditions with active control. As part of the revision process of the Ecodesign and Energy Labelling regulations, BAM proposed in 2019 [1] to make the compensation method mandatory with the new regulations to adapt the test standards to the the state of development in heat pump technology and leverage savings potential.

BAM subsequently conducted two large round robin tests [3] to validate the compensation method. It was found that the inertia of the test rig, in particular, must be specified and aligned among test laboratories to achieve reproducible results under part load conditions. The inertia's influence on the heat pump's operating behavior was proven in a parameter study in cooperation with the RWTH. [4] In another study it could be shown for three laboratories that by adjusting the test stand inertia, more reproducible results could be achieved than in the round robin test test. [5] In order to be able to continue using existing laboratory infrastructure, the inertia is ideally emulated on the control side (technology-neutral). For this purpose, BAM and RWTH have developed a representative building model that can be integrated into the test bench control and ensures that (a) all test benches and laboratories react physically in the same way (aligned inertia) and (b) representative, reproducible test results are achieved, especially at partial load. The practical implementation and interaction of different heat pump controllers with the extended test bench controller is a current research subject and is being investigated in this project.

By integrating the heat pump controller into the test using a building model, any control strategies can be compared for the first time regarding energy efficiency (fixed vs. variable mass flow, outdoor temperature vs. indoor temperature guided control, etc.), and a level playing field is created. The coupling of a virtual building with a heat pump through the test bench is already known from hardware-in-the-loop (HiL) methods. [6] However, the focus of these investigations is on the overall system consisting of the heat pump, heating system, and building. Transferring the principle to product testing under standardised conditions is challenging and new. The integration of a building model into the test serves, on the one hand, to ensure equal test rig inertia and, on the other hand, offers the possibility to further develop the methodology in the future in order to test advanced heat pump controllers, for example, under dynamic load changes (e.g., simulation of solar irradiation). New controller concepts are becoming increasingly important with rising insulation standards

Several groups worldwide are working on comparable test methods (Waseda University in Japan, Purdue University in USA, CSA EXP07 in Canada and IEA 4E air conditioner project 2.0). However, the focus is on air-to-air units that are tested on different test rigs. The project partners are not aware of any project worldwide that develops standardised load-based test procedures for water-based (vertical) heat pumps.

The project's overall objective is to create the prerequisites to establish the compensation method at EU level to achieve the following improvements: (a) Through representative, reproducible, and independent testing, design incentives are set to optimise heat pump systems holistically (incl. controllers) and to maximise energy efficiency. According to an estimation by the NGO CLASP [7], maximising energy efficiency by introducing the compensation method can achieve savings up to 340 TWh by 2050 and a sustainable reduction in environmental impact. (b) Realistic testing and reliable evaluation of heat pumps will also increase consumer acceptance. Furthermore, uniform test conditions allow a fair comparison of technologies so that the energy label can provide good guidance to consumers when choosing efficient appliances. Finally, (c) conformity is ensured by independent market surveillance which becomes inceasingly important in light of the large scale roll-out of heat pumps.

The negotiations on the EU regulations are expected for early 2024. The final decision will then be made as to whether the compensation method will be introduced mandatory and whether the outlined environmental benefits can be realised in the near future. Against this background, the research project validates the method development in the form of a feasibility study. The results are to be communicated to the EU Commission, Member State representatives, and stakeholders and are used as a basis for decision-making in the upcoming negotiations. Furthermore, the results will be introduced into CEN/TC 113/WG 8 and are intended to accelerate the standardisation work on the compensation method.

Specifically, in this research project (proof-of-concept), the feasibility of the new test method (incl. building model) is demonstrated on three heat pumps from different manufacturers in three test institutes with different laboratory infrastructures. Test benches with and without intermediate circuits are selected. The investigations focus on the interaction of the test bench and heat pump controller. Common control concepts are investigated (variable vs. fixed mass flow, outdoor temperature guided control), and more recent concepts that are increasingly integrated into heat pump controllers (indoor temperature guided control). Furthermore, the influence of permissible deviations on the key performance indicators (COP and SCOP) is estimated through repeated measurements with targeted parameter variations (e.g., targeted deviation of the return temperature from the setpoint).

3. Building model integration

Integrating a building's inertia into testing procedures requires a building simulation model. The building model computes the behaviour of the building, which must be emulated at different test

benches (labs 1-3 in this study). The simplified building model (section 3.1) is described by only six equations, which are covered in a Phython script[1], for example. The script can be integrated into the individual test stand's software. The Python implementation is developed by RWTH to align the model integration and parameterisation. In the context of this project, all labs use the developed Python implementation successfully. The interaction between the Python program and the test bench software is realised individually. As an example, RWTH uses a cloud-based system with the data protocol MQTT for this purpose. The following section describes the building model in more detail.

3.1. Building model

The simplified building model (two-mass model, cf. Figure 1) computes the return temperature $\vartheta_{\mathrm{R,calc}}$ (and the building temperature $\vartheta_{\mathrm{B,calc}}$, where applicable) which is coming from the building towards the heat pump. The test stands emulate the(se) computed temperature(s) during the entire test duration. A schematic is shown in Figure 1.

In particular, for each time step Δt_{step}, the model calculates the return temperature $\vartheta_{\mathrm{R,calc}}$ and the building temperature $\vartheta_{\mathrm{B,calc}}$ (output variables) based on the measured supply temperature ϑ_S and the heating capacity $\dot{Q}_{\mathrm{HP}}$ (input variables) of the unit under test. Through the measured heating power, the model considers the supply temperature ϑ_s, return temperature $\vartheta_{\mathrm{R,emu}}$, and mass flow rate $\dot{m}_{\mathrm{W}}$. Like the supply temperature the mass flow is controlled by the heat pump.

Based on a simple energy balance, the test stand dynamically adapts the so-called compensation load to match the calculated return temperature $\vartheta_{\mathrm{R,calc}}$. The heat pump responds in accordance using its heating curve or its indoor temperature control or both as it tries to maintain the required supply temperature ϑ_s. Aligned with testing conditions in EN 14825, the outdoor room shall maintain constant conditions over a temperature range associated with different climate zones for testing air-water heat pumps. Compared to the conventional testing procedure, the heat pump under test is operated with its onboard control system (native control) active and not in a fixed-speed mode. The heat pump is, thus, permitted to switch into on/off operation of the compressor.

To ensure representativeness the building model is parameterised according to the test conditions defined in EN 14825 taking into account the temperature application (e.g. low or medium) and the climate zones (cold, average, warm). In addition, the P_{design} of the heat pump is considered to scale the size of the virtual building. The equations and a detailed description can be found in the test guideline published on the BAM website[2].

[1] https://github.com/BAMresearch/bam-load-based-testing
[2] https://netzwerke.bam.de/Netzwerke/Content/DE/Downloads/Evpg/Heizen-Kuehlen-Lueften/bam%20test%20guideline%20-%20load-based%20testing%20of%20heat%20pumps%202023.pdf.html

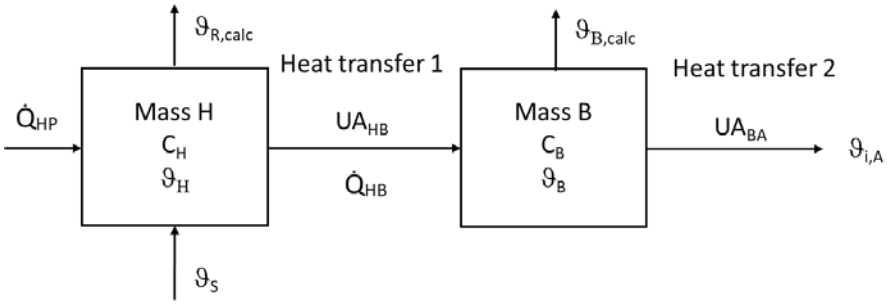

Figure 1: Schematic of the two-mass building model.

3.2. Test stand modifications

In contrast to steady-state testing, the dynamics in load-based tests generally pose higher requirements on the test stands. To assess the control limits of existing test stands and propose suitable modifications, two common test stand designs were included in this study besides the test rig at RWTH.

In the first project phase, the three labs prepared their test infrastructure to emulate the return temperature using the two-mass building model. All three labs used the Python script provided by RWTH and implemented it in their test stand control.

Due to the sophisticated Hardware-in-the-Loop (HiL) infrastructure at RWTH (lab 1) no hardware changes were made to the admixing circuit (direct method) of the test stand and the PID settings of the controllers were not changed. However, the measurements revealed that the test stand cannot compensate for load changes with very high dynamics during defrost and the return temperature falls below the calculated setpoint. During defrosting, the test stand must switch between heating and cooling within a few seconds, which is currently not possible for all test stands (section 4.1). To capture all relevant operating modes that account for the heat pump's efficiency in the field, the defrost operation must be properly integrated into the testing procedure. Therefore, it was considered to modify the test stand to allow cooling and heating based on the heat pump operating mode. The impact of this modification on the repeatability of test results will be investigated in the planned round-robin test to possibly revise the permissible deviations on defrost and ensure meaningful testing and evaluation of the key performance indicators.[3]

Lab 2 (Austrian Institute of Technology, AIT) has a test stand with intermediate circuit, connecting the heat pump and the primary cooling circuit of the lab. A parallel plate heat exchanger is used to apply the cooling load. After implementing the python script in the test stand control, most of

[3] It has been shown after the project end that installing a small buffer tank of about 20 litres (for test points with defrost operation) behind the heat pump's water outlet added enough "physical" inertia to solve the issue. No additional heating function was required to respect the permissible deviations during defrost. Therefore, this approach is a suitable low-cost option for labs that have no heating function on their test rig yet. Details will be published within another DBU funded project (38943/01).

the effort was spent to tune the PID settings of the valves to reduce oscillations from the set return temperature caused by the inertia of the intermediate circuit (heat exchanger, water volume).

Lab 3 (ILK Dresden) also used the direct method. Therefore, implementing the building model in the test stand control is straightforward since a setpoint for the return temperature is already calculated and, in their common practice, only the equations must be replaced. A schematic and a picture of the test rig is shown in Figure 2. In principle, the test stand consists of a rather simple mixing station (with a controllable three-gate valve) between the heat pump and the primary cooling circuit of the lab. In the course of the project, an electrical heater was added in the water loop of the test stand to allow for better controllability when compensating sudden load changes during defrost, as discussed above. Building a new test stand dedicated to compensation measurements is therefore not very costly. Since existing infrastructure can usually be adapted an introduction of the compensation method would not result in huge investments for most labs.

Finally, the implementation of the building model on both the hardware and software was realised in three weeks by lab 2 and lab 3. Considering that the labs had no experience in HiL testing, a few weeks or months should be sufficient for other labs to prepare their test rigs for compensation method measurements.

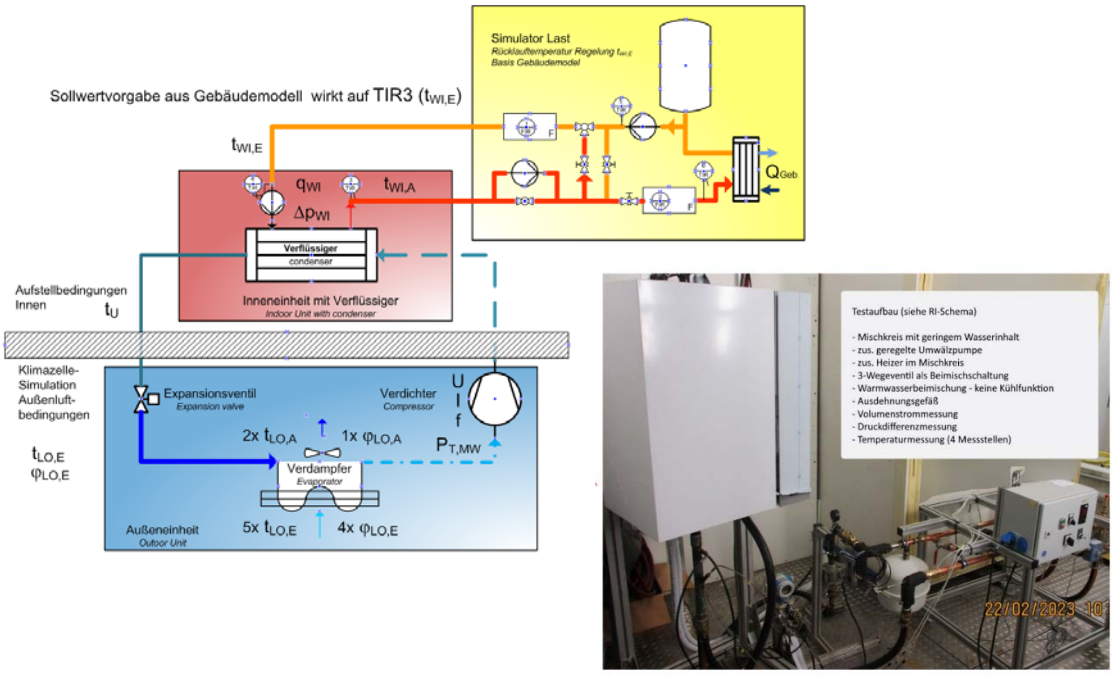

Figure 2: Schematic of the test stand with admixing circuit (direct method) of lab 3.

3.3. Pre-tests

After fully integrating the two-mass building model, lab 2 performed a pre-test with changing load conditions to check the building model response for plausibility. For this the P_{design} value in the Python script was changed during the measurement. Figure 3 shows the time series of the measurement and Table 1 summarises the parameter changes made to the building model during the test. The pre-test was performed with HP2 at +7 °C outdoor temperature and a supply temperature of 36 °C.

The test starts with a P_{design} of 21 kW (set in the Python script) resulting in a part-load capacity of 7.3 kW for the selected test condition. At 18:30 the P_{design} in the building model was changed to 15 kW lowering the part-load capacity to 5.3 kW. The calculated return temperature set point increases accordingly since the supply temperature stays at the setpoint defined by the heating curve (top graph of Figure 3). Hence, the temperature spread between supply and return temperature decreases and the heating capacity follows the building load (compare heat fluxes, bottom graph of Figure 3). Similar observations are made at 19:55 when P_{design} was lowered to 11.4 kW.

With the next adjustment of P_{design} (8.6 kW) at 20:41 the part-load capacity becomes so low (3.0 kW) that the minimum compressor frequency is reached (modulation limit) and the provided heating capacity is slightly too high compared to the building load (compare heat fluxes, bottom graph of Figure 3). Consequently, the supply temperature starts to raise and the building model increases the setpoint for the return temperature. In parallel, the heating system's temperature (mass H) in the building model raises. In contrast, the calculated building temperature stays constant within the rather short measurement period because the higher mass of the building (mass B) dampens the temperature increase. Lowering the P_{design} even further (5.7 kW) makes the mismatch between provided heat and building load much more apparent. The supply, return and heating system temperatures raise much steeper until at 22:13 T_{supply}=39 °C and the heat pump controller shuts off the compressor (P_{el}=0). The supply temperature drops and follows the calculated set point of the return temperature shortly after the compressor stopped (zero temperature spread) since the heat pump provides no heat anymore. Finally, at 22:40 when the supply temperature dropped below 32 °C the controller restarts the compressor. As expected, the heat pump now operates in on-off cycling because of the low load conditions.

The pre-test shows realistic interaction between heat pump and test stand as expected under field conditions with a changing building load. Therefore, it was decided to start the tests described in the following sections to study the interaction of the different heat pumps with the different test rigs under different test conditions.

Table 1: P_{design} changes made in the building model at different measurement times and resulting part-load capacities P_h during the pre-test at PLR C in lab 2 (Figure 3).

Time	P_{design} [kW]	P_h [kW]
17:00	21.0	7.3
18:30	15.0	5.3
19:55	11.4	4.0
20:41	8.6	3.0
21:57	5.7	2.0

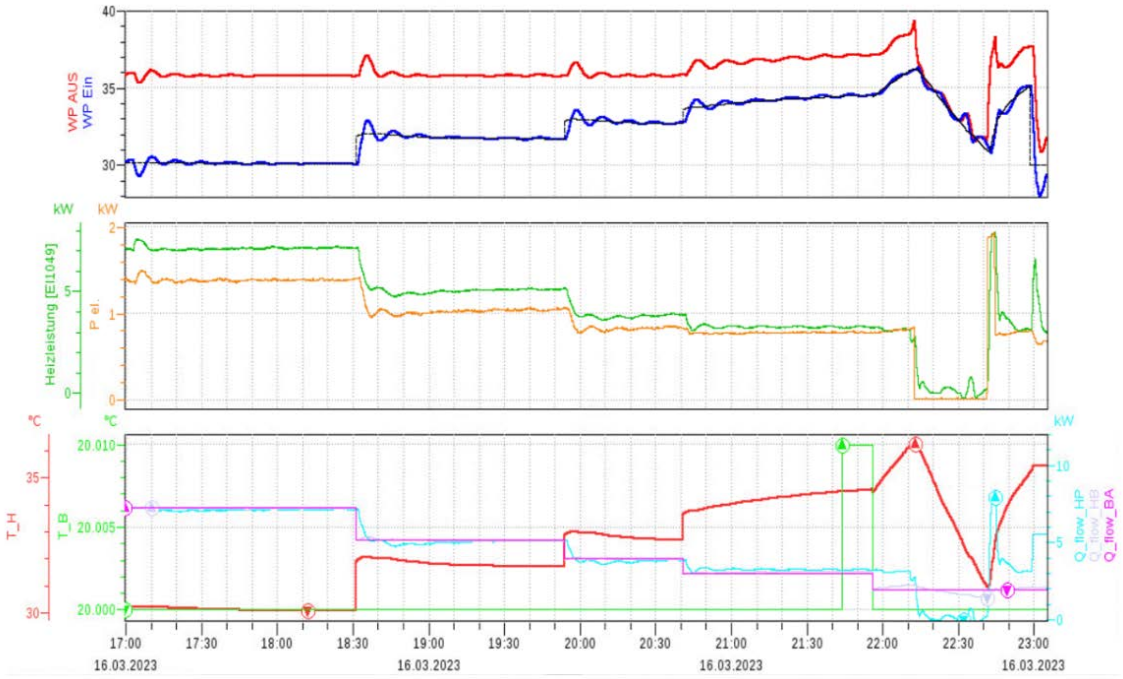

Figure 3: Pre-test with PLR C (fixed flow setting of HP2) in lab 2 with different P_{design} values and resulting part-load capacities listed in Table 1; Top: supply (red) and return (blue) temperatures, calculated set return temperature (black); Center: heating capacity (green) and electrical power input (orange); Bottom: calculated temperatures for mass H (red) and mass B (green), calculated heat fluxes between heat pump and mass H (cyan), between mass H and B (light gray), mass B and the ambient (purple).

3.4. Step response

In contrast to former standardised test methods with fixed compressor speed, load-based testing methods result in higher dynamics, particularly in low part load conditions leading to cycling behaviour, which is observed in field test operation as well. High dynamic heat pump operation leads to higher requirements for the test labs. In particular, the requirements for hydraulic temperature control are increasing. Pre-tests can estimate whether the test bench fulfils the higher requirements. High gradients of the set temperature occur after a compressor stop. Therefore, step responses are measured in each lab to guarantee that the test bench can follow the calculated set temperature of the two-mass model. The step response test is performed as follows:

1. Steady-state heat pump operation with coupled two-mass model (test point A or test point E)
2. Stop heat pump operation by switching off heat pump manually but guarantee volume flow through the test bench.
3. Room temperature and transfer system temperature decrease, wait until at least 2/3 of the step response (appr. 45 °C → 20 °C) is fulfilled.
4. Evaluate the deviation between the return temperature and the return set temperature.

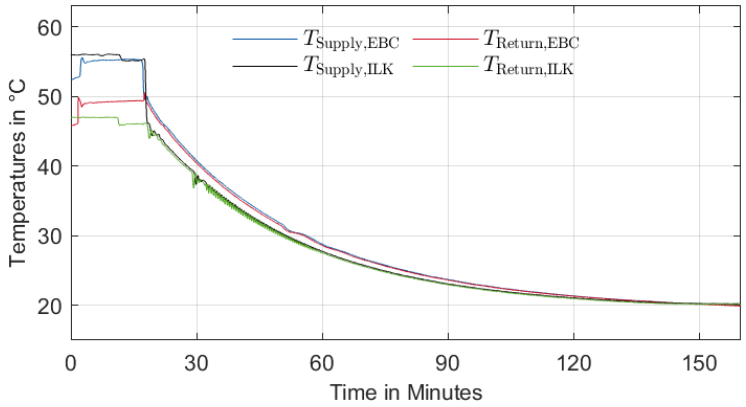

Figure 4: Supply and return temperature during performed step response by lab RWTH (EBC) and ILK

Figure 4 compares the step response experiments of lab 3 (ILK) and lab 1 (RWTH). Both tests are performed with different heat pumps but the same two-mass building model. In general, both curves show similar behaviour. During the steady-state heat pump operation within the first 20 min, the supply temperatures are at the same temperature level of 55 °C. The return temperature at EBC and ILK is about 50 °C and 47 °C, respectively. The slightly lower return is heat pump dependent and conditional on different volume flows. The building and the transfer system cool down after turning off the heat pump. Both labs can follow the specifications and show stable control behaviour.

Lab 2 performed the step response test before the other labs. Therefore, a previous version of the python script was used, which still included fixed values for the heat transfers and the heat capacities in the two-mass building model. This was replaced in the later version of the script, used by lab 1 and lab 3, by a single time constant to ensure the same inertia for all P_{design}. The difference in the building models results in different inertia and, thus cooling behaviour during the step response. However, lab 2 managed to control the return temperature close to the setpoint (< 0.5 K). Only during the initial phase of the step response, where the sudden load change occurs, the deviation was slightly higher (about 1 K). Based on this observation and the pre-tests described in section 3.3 it was decided not to repeat the measurement since Lab 2 test bench is able to handle the dynamic return temperature.

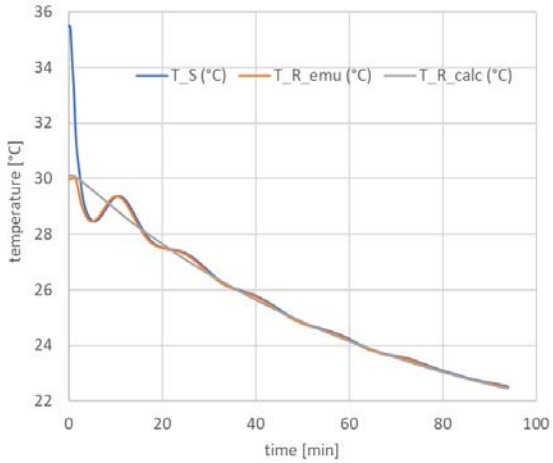

Figure 5: Supply temperature, emulated and calculated return temperature during step response of lab 2. Start condition corresponds to test point E (low temperature application).

4. PoC – Test results and discussion

The following section shows and discusses test results obtained after successfully implementing the two-mass model on the three test rigs (lab 1-3). Each lab tested a different heat pump (HP1-3) to prove the feasibility of the revised methodology for different controllers of different manufacturers. The labs performed measurements under the five test conditions E, A, B, C and D described in EN 14825:2022 for the medium temperature application and the average climate (55 °C supply temperature at full load). The part-load conditions were calculated using the P_{design} declared by the manufacturer. The two-mass model parameters used for the tests are given in the test guideline published by BAM. The compensation measurements were performed according to the same guideline.

The main focus is on the operation behaviour of the tested heat pumps to assess whether the interaction of the test stand and heat pump controllers yield representative results. Additionally, the COP and $SCOP_{on}$ are calculated from the compensation measurements performed by lab 1 and lab 2 and compared to the declared key performance indicators measured according to EN 14511 and EN 14825. To evaluate the COP under bivalent operating conditions, both labs 19ctive the electrical back-up heater during the test. The current standards do not include the back-up heater in the test. According to EN 14825 the electrical power input of a fictive back-up heater is added in the $SCOP_{on}$ calculation for each part load assuming a COP of 1. However, this procedure cannot be applied to the compensation method: For outdoor temperatures below T_{biv} the heating capacity of the heat pump cannot cover the building load and the building temperature would continuously decrease. Therefore, the test would become unstable and subsequent defrost cycles would become non-reproducible, for instance. An alternative approach is to activate the physical back-up heater during the test as studied by lab 1 and lab 2

(section 4.2.2).[4] The electrical back-up heater compensates the deficit in heating power and its electrical power input is directly measured. Furthermore, the backup heater's controller strategy is part of the measurement. In principle, this should yield more representative operating behaviour and test results.

4.1. Lab 1 – RWTH

The device under test is an air-to-water heat pump with a design heating capacity of about 10 kW. The methodology with the novel 2-mass model aims at testing heat pumps under realistic and reproducible conditions. Therefore, the heat pump under test works in a standard mode with a configured heating curve that fits the conditions of EN 14825:2022 for the medium temperature application.

4.1.1. Heating curve and fixed flow

Figure 6 and Figure 7 show measured and calculated temperatures and heat flows for test points A, B and C, D, respectively. According to the test guideline, at least three reproducible cycles were recorded.

PLR A and PLR B

Under test condition A, the heat pump operates in two different cycles characterised by a heating and defrosting period. Two cycles with a maximum supply temperature of 52 °C follow a cycle with a maximum supply temperature of 56 °C. While only the heat pump operation is observed during the lower temperature cycles, the heat pump uses the additional electrical back-up heater within the higher temperature cycles. Therefore, the test period includes three cycles with back-up heater operation.

The heat flows (Figure 6, center) show different dynamics. While the heat flow $\dot{Q}_{\mathrm{HP}}$ has a high dynamic behaviour, the heat flow $\dot{Q}_{\mathrm{HB}}$ changes in a small range, and the heat flow $\dot{Q}_{\mathrm{BA}}$ is almost constant. This behaviour can be explained by the additional inertia through the two-mass model. The virtual building temperature (temperature of mass B) could be almost kept constant through the heat pump operation. However, defrost operations decrease the building temperature, leading to a slightly lower building temperature after the whole test. Differences between the building temperature and the desired temperature of 20 °C indicate that the heat pump does not reach the design heat load in realistic test conditions.

[4] Meanwhile the concept of a virtual back-up heater has been successfully tested within the round robin test (RRT) on the compensation method (DBU 38943/01). The virtual heater has been implemented in the python script and compensates any difference between measured and set heating capacity during the measurement. To achieve representative operating behaviour of the unit under test the power of the virtual heater is limited to the maximum declared power value of the real back-up heater. Detailed results will be published in the project report covering the RRT.

Compared to the standardised test (EN 14511), defrost operation was obtained in test point A. Additionally, the test procedure (two-mass model) shows reproducible heat pump behaviour, although the heat pump operates in heating, booster, and defrost modes.

In test point B conditions (Figure 6, right-hand side), the heat pump operates in heating and defrost mode. This behaviour is typical for these conditions and is generally also measured in standardised tests according to EN 14511. The results show three reproducible cycles consisting of a heating and a defrosting period. The building temperature slightly increased during the test because of too high average supply temperatures. For future tests, the heating curve must be adjusted.

PLR C and PLR D

Figure 7 illustrates the test points under part load conditions C and D, leading to cycle operation. In contrast to test points A and B, defrosting is no longer present at points C and D. Instead, the heat pump switches the compressor off because the heat pump's modulation limit is reached (lowest possible compressor speed). Both tests show a reproducible cycling behaviour. The emulated building temperature increases slightly over the test period, indicating too high average supply temperatures. In future tests, the heating curve has to be adjusted iteratively until the average supply temperature fits the setpoint. In test point D, all specifications are met, and the heat pump heats the virtual building to a constant temperature of 20 °C. In test point D, the cycles' lengths are about one-third compared to test point C. Heat pumps can only influence the average heating capacity during these very low part load conditions by adjusting their cycling behaviour. While the heat pump runs for about 45 minutes and is off for about 15 minutes in test point C, the heat pump runs in test point D for only 5 minutes. Compared to EN 14511, which keeps the compressor speed fixed during the test, the heat pump cycles under realistic conditions given in these tests due to the two-mass model.

In summary, all test points could be tested under realistic conditions with the help of the two-mass model. The heat pump operates either in defrost cycles or part load cycles, indicating a high dynamic that must be defined for standardised testing. The virtual room temperature shows an intelligible value for the heat pump test and can be used as an input value for higher control systems. The average supply does not fit to the specifications in all test points. This indicates that the heat pump does not accurately follow the given heating curve. For a comparable, standardised measurement, the heating curve must be iteratively adjusted to the setpoint temperature in the future.

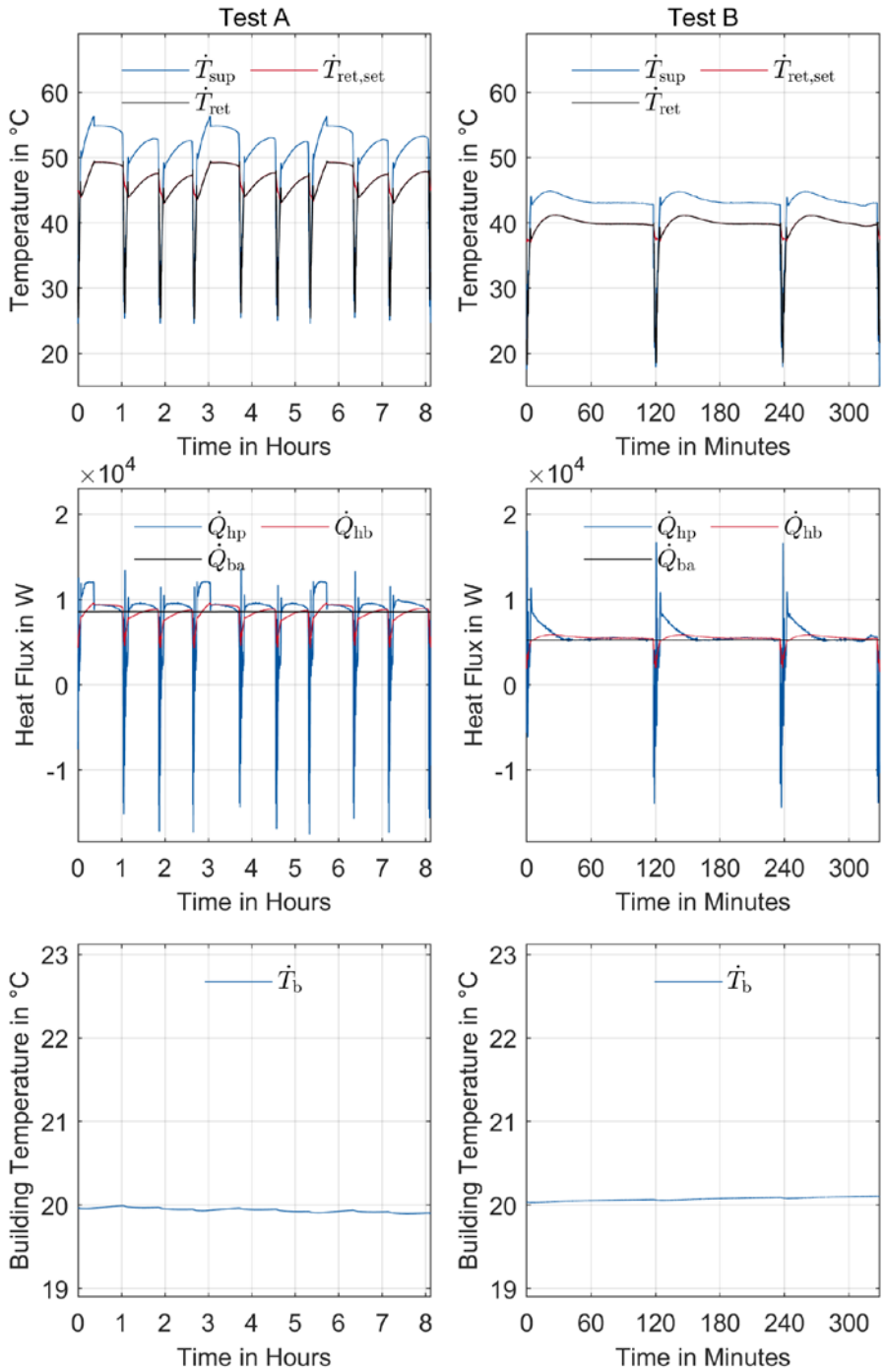

Figure 6: Heat pump operation with the two-mass model for test points A and B; Top: supply temperature ϑ_s (here: T_{sup}), return temperature ϑ_r (here: T_{ret}), and return set temperature $\vartheta_{R,calc}$ (here: $T_{ret,set}$); Centre: heat flow from heat pump into mass H $\dot{Q}_{HP}$, heat flow from mass H into mass B $\dot{Q}_{HB}$, heat flow from mass B into the environment $\dot{Q}_{BA}$; Bottom: temperature of virtual building $\vartheta_{B,calc}$ (here: T_b).

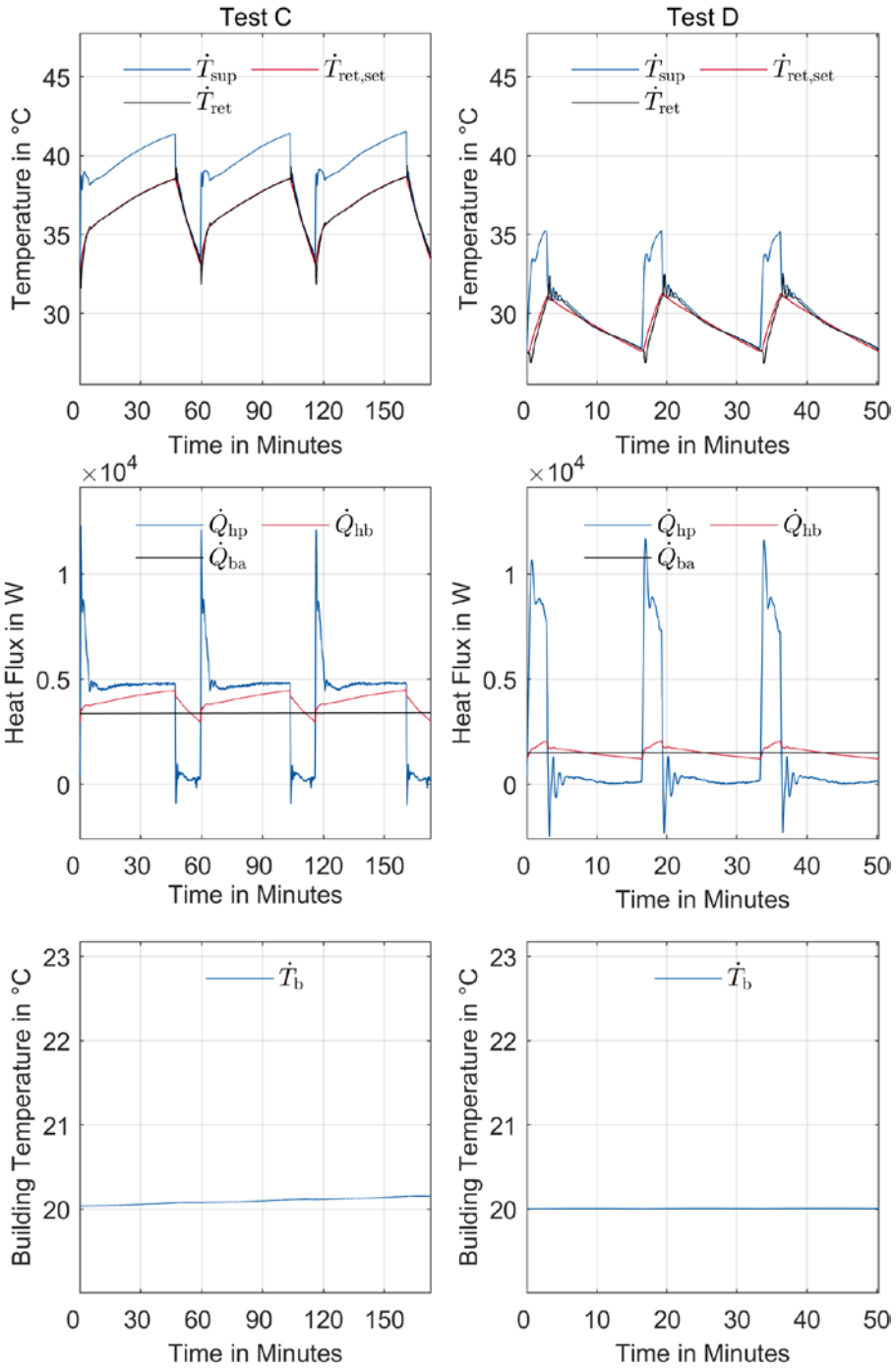

Figure 7: Heat pump operation with the two-mass model for test points C and D; Top: supply temperature ϑ_s (here: T_{sup}), return temperature ϑ_r (here: T_{ret}), and return set temperature $\vartheta_{R,calc}$ (here: $T_{ret,set}$); Centre: heat flow from heat pump into mass H $\dot{Q}_{HP}$, heat flow from mass H into mass B $\dot{Q}_{HB}$, heat flow from mass B into the environment $\dot{Q}_{BA}$, Bottom: temperature of virtual building $\vartheta_{B,calc}$ (here: T_b)

4.1.2. Electrical back-up heater

The electrical backup heater of HP1 turns on for temperatures below the bivalence point. In all tests within this project the bivalence point is equal to test point A resulting in an ambient temperature of 7 °C. Additionally, the backup heater turns on depending on the manufacturer's control strategy for instance during defrost operation.

During all performed tests the back-up heater was generally activated but only turns on in test point E and A. Figure 8 and Figure 9 show the electrical power consumption of the heat pump and the back-up heater in test point A and E, respectively. Since the ambient temperature of test point E is below the bivalence point and the heat pump cannot reach the necessary heating load and supply temperature the backup heater runs during the whole test with a constant heating load of 3 kW.

For test point A the heat pump can follow the set point for the heating capacity during period H (heating period). However, due to frequent defrost operation the design heating capacity cannot be reached in average over period H and D (defrost period). The heat pump activates the back-up heater in every third cycle (compare with Figure 9) resulting in reproducible operating behaviour.

Generally, both test points (A and E) show that the compensation method with the two-mass model can be used with a physically activated back-up heater. In addition, the tests represents real-life operation of heat pump systems and thus integrate the control strategy of the back up heater into the standardised KPI (COP).

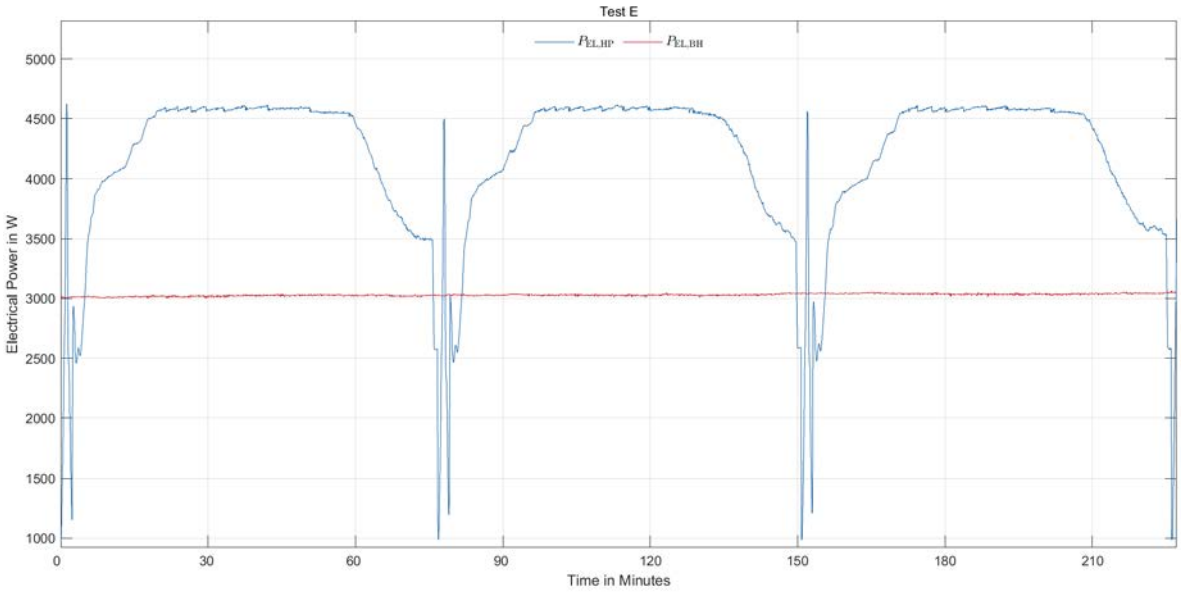

Figure 8: Electrical power consumption of HP1 and the activated electrical back-up heater in test point E.

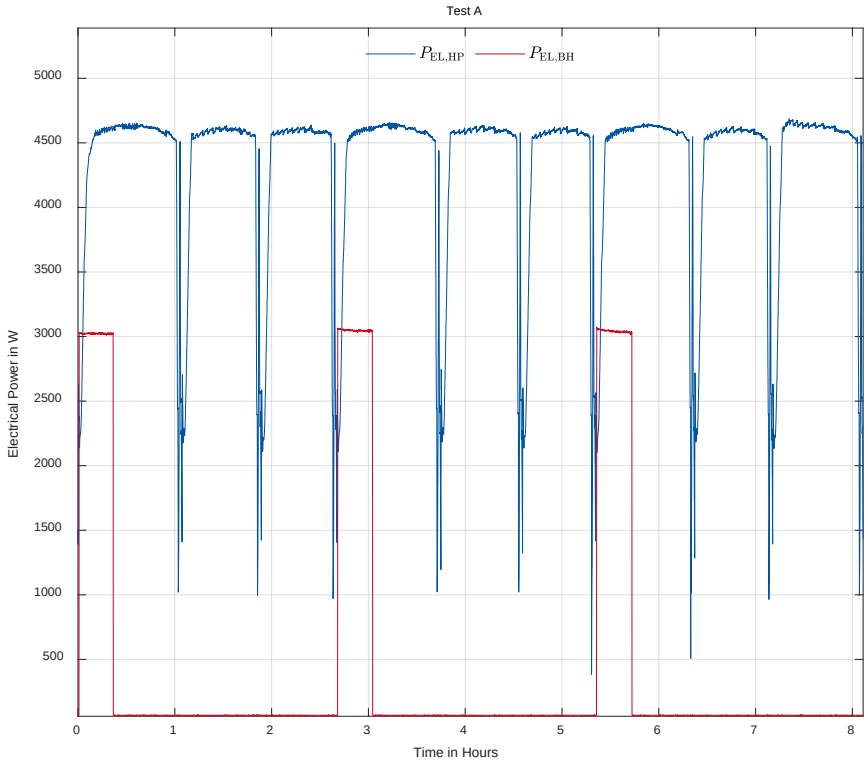

Figure 9: Electrical power consumption of HP1 and activated electrical back-up heater in test point A.

4.1.3. COPs and $SCOP_{on}$

This section discusses the results of the conducted experiments by comparing the COPs and $SCOP_{on}$ with the declared values according to the current standard EN 14511.

Table 2 summarises important parameters of all conducted experiments with HP1. First, the backup heater was only in use during PLR E and PLR A. The average supply temperature ϑ_s does not fit in every test point to the setpoint according to EN 14825. While the temperatures for test points B and D fit well (deviation <1 K), the average supply temperature is too high in test point E and C and to low in test point A. The reason for the deviation between both temperatures are due to the simple control strategy of the heat pump which does not take the defrost period or on/off behaviour into account. In general, the heating curve has to be adjusted until the temperatures fit to the setpoint. In context of this work (proof of concept) a repetition is not conducted.

The return temperature which is controlled by the test bench fits to the emulated return temperature. Only in test point E, A and B small deviation can be observed. Deviations only occur during period D (defrost period) where the heat pump switches from heating to cooling mode. This results in a heat demand instead of a cooling demand from the test bench's perspective. These problems can be solved by an additional buffer tank in the supply pipe (behind the outdoor

heat exchanger water outlet) or an additional heating element inside the test bench which is successfully demonstrated in the next project phase (38943/01).

Comparing the measured COP with the declared COP values according EN 14511 is difficult due to the deviations between measured and set supply temperature. Furthermore, for all COP values measured according to the compensation method, the total electrical consumption (heat pump and backup heater) is taken into account whereas the declared COP considers only the consumption of the heat pump. According to EN 14825 the electrical consumption of a virtual back-up heater is only considered in the SCOP calculation. Thus, for test conditions where the declared heating capacity is too low the COPs of both methods are not directly comparable. For HP1 this is the case for PLR E. However, a few facts can be observed:

- Although the supply temperature in PLR A is lower than the setpoint, the measured COP is below the COP according to EN 14511. The reason might be that in EN 14511 measurements, no defrost occurs, whereas defrost cycles occur during compensation measurements with the activated controller. Additionally, the backup heater turns on after every third defrost operation. Both effects decrease the efficiency and, thus, the COP.
- For very low part load conditions (PLR D) the declared COP according to EN 14511 is much higher than the one measured according to the compensation method. The degradation factor used to correct for cycling of the compressor is probably not representative.

We use the $SCOP_{on}$ calculated according to EN14825 to compare the annual KPI of both methods. The resulting $SCOP_{on}$ for the compensation method and the declared value is 2.74 and 3.41, respectively. Since the $SCOP_{on}$ calculation is based on the COP values, the above arguments can explain the differences.
The results underline the need for representative test methods to provide realistic performance indicators to planners, installers and customers.

Table 2: Average temperatures, heating load and efficiency (COP) for all test points.

	PLR E	PLR A	PLR B	PLR C	PLR D
Condition	A-10W55	A-7W52	A2W42	A7W36	A12W30
Evaluation period	3 defrost cycles	9 defrost & 3 backup heater cycles	1 defrost cycle	70 min	4 on/off cycles
BU heater in use	yes	yes	no	no	no
ϑ_s [°C]	56.1	50.8	42.8	39.1	30.2
$\vartheta_{s,set}$ [°C]	55	52	42	36	30
$\vartheta_{R,calc}$[°C]	50.5	46.7	40	36.7	29.3
$\vartheta_{R,emu}$ [°C]	50.1	45.8	39.5	36.7	29.3
Q_{HP} [kW]	10	8.42	5.46	4.01	1.54
COP	1.39	1.77	2.78	3.47	3.62
COP (EN14511)	2.1	2.3	3.2	4.4	5.9
$SCOP_{on}$ (Comp.)			2.74		
$SCOP_{on}$ (EN14511)			3.41		

4.2. Lab 2 – AIT

Lab 2 performed measurements on an A/W heat pump with a declared heating capacity of 15 kW. In contrast to the other two labs a test stand with intermediate circuit was used. All measurements were performed with a constant flow rate. In addition, to the five test points A to E further tests were performed with active electrical back-up heater of HP2.

4.2.1. Excluding back-up heater

PLR E

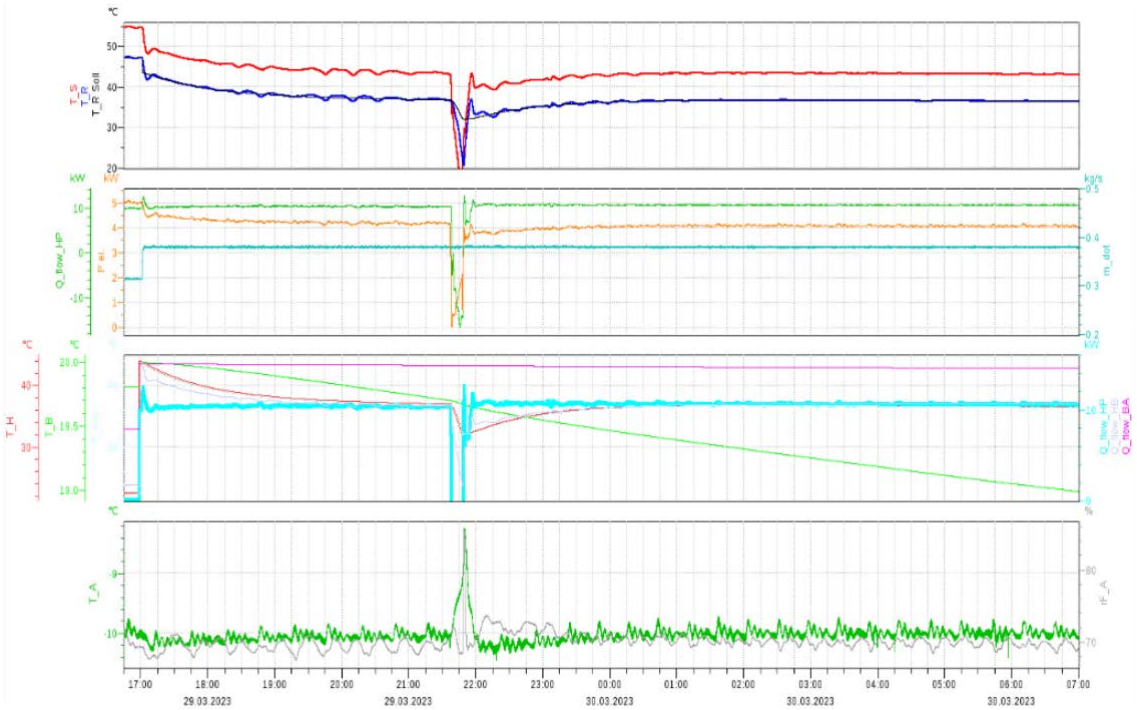

Figure 10: Time series of measured and calculated parameters at PLR E; Top: supply temperature (red), return temperature (blue), set return temperature (black); centre top: heating capacity (green), electrical power input (orange), mass flow rate (cyan); Centre bottom: temperature of mass H (red) and mass B (green), heat fluxes between heat pump and mass H (cyan), mass H and mass B (light grey), mass B and the ambient (purple); Bottom: outdoor temperature (green), relative humidity (grey).

Figure 10 show the operation behaviour of HP2 under test condition E with the declared P_{design} of 15 kW. At 17:00 the building model was activated leading to a sudden change of the set return temperature to 43.6 °C which is then calculated by the building model based on P_{design}. Here after the supply temperature decreases until it stabilises between 19:00 and 20:00 resulting in a heating capacity of about 10 kW instead of the required 15 kW. Similar to HP3 the manufacturer of HP2 declared a rather high P_{design} for the unit with a bivalence temperature higher than -10 °C (outdoor temperature of test point E). Since the included electrical back-up heater is not activated during this test the building temperature drops over the measurement period from 20 °C to 19 °C. Around 21:45 a defrost process is initiated by the heat pump controller followed by a long period of steady state operation.

Prior to testing it was unclear whether the test stand with intermediate circuit would be fast enough to control the return temperature close to the calculated setpoint. However, the measurements show that the test bench is capable to follow the setpoint rather well. Only during defrost the return temperature drops below the set temperature. As discussed for lab 1 and lab 3 this could be fixed by adding an electrical heater in the water loop of the test stand for better controllability of the return temperature.

PLR A

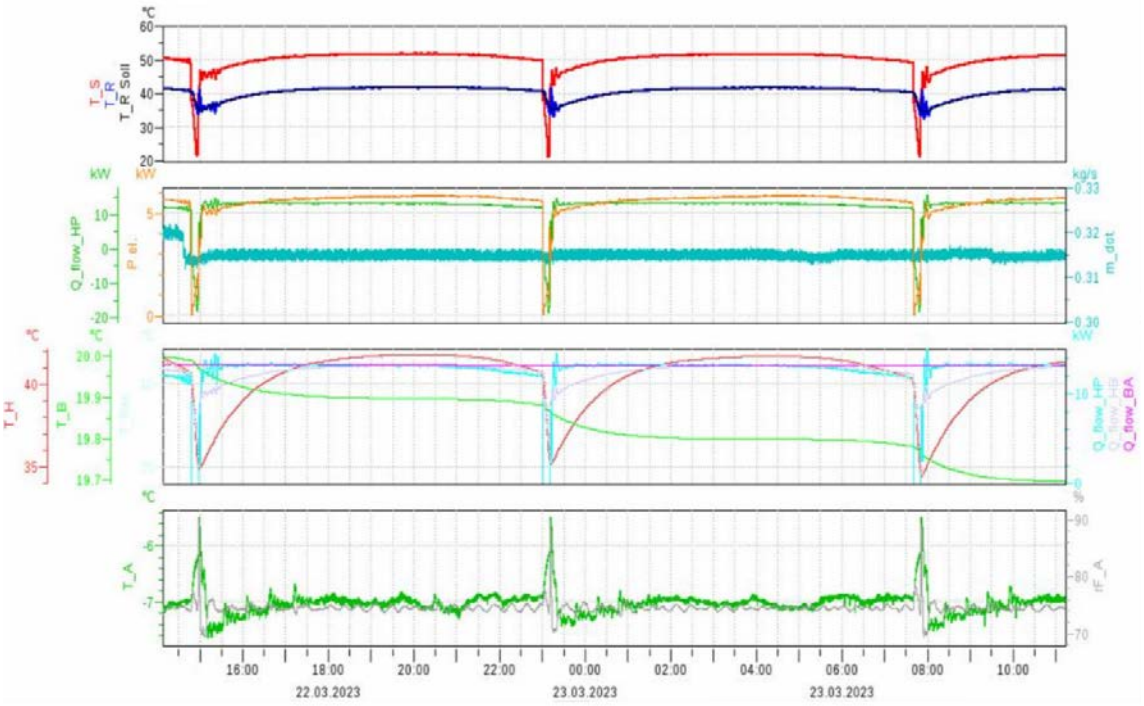

Figure 11: Time series of measured and calculated parameters at PLR A; Top: supply temperature (red), return temperature (blue), set return temperature (black); Centre top: heating capacity (green), electrical power input (orange), mass flow rate (cyan); Centre bottom: temperature of mass H (red) and mass B (green), heat fluxes between heat pump and mass H (cyan), mass H and mass B (light grey), mass B and the ambient (purple); Bottom: outdoor temperature (green), relative humidity (grey).

Figure 11 shows the operating behaviour of HP2 under PLR A with the declared P_{design} of 15 KW. Similar to PLR E defrost operation is observed at 17:00 and 03:00. Also, the return temperature follows the set point rather well. In contrast to PLR E the return temperature can be kept close to the setpoint even during defrost operation. The reason might be related to the lower cooling load applied by the test stand at test condition A compared to E. Obviously, the test stand controller is still able to compensate the instantaneous smaller load changes at PLR A but not the higher load changes at PLR E anymore. Nevertheless, the return temperature oscillates with an initial amplitude of 5 K around the set point during defrost at PLR A. Adding an electrical heater in the test stand water loop is likely to improve the controllability, as discussed before.

Despite adjustments of the heating curve, the supply temperature averaged over a full defrost cycle (period D and H) equals 50.1 °C and is about 2 K lower than the setpoint of 52 °C. The reason is a too high declared heating capacity resulting in a bivalence temperature above -7 °C. Additional measurements (not shown) confirmed that the setpoint for the average supply temperature could be reached with a lower P_{design} of 13.5 kW.

PLR B

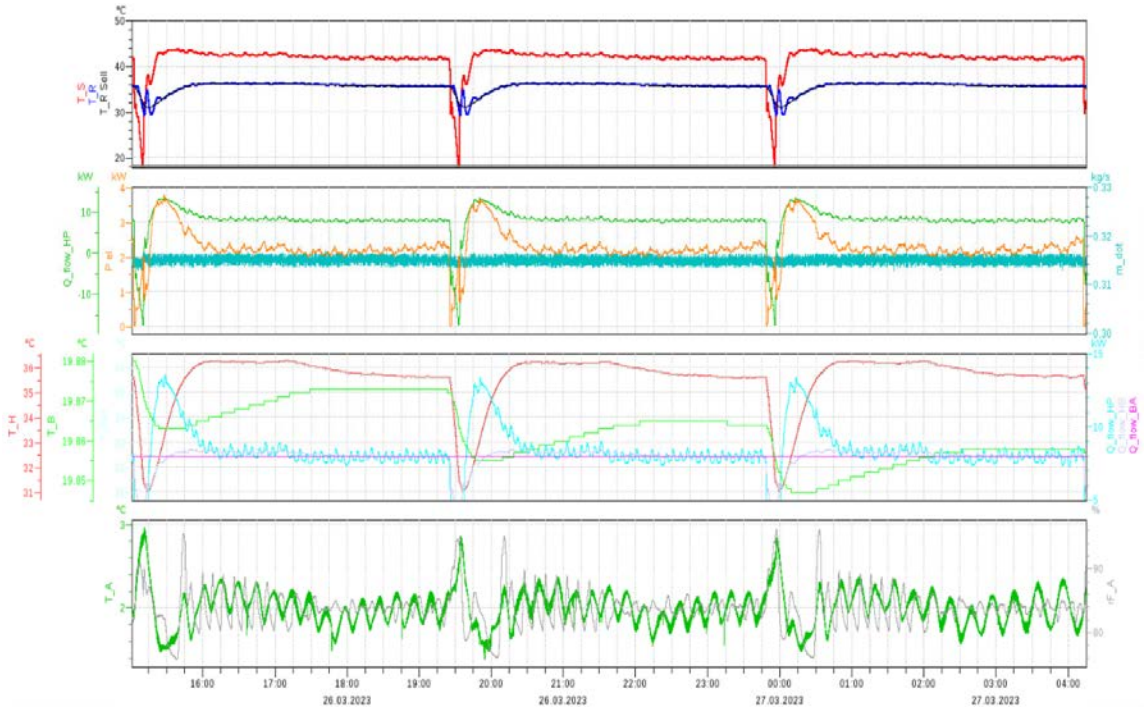

Figure 12: Time series of measured and calculated parameters at PLR B; Top: supply temperature (red), return temperature (blue), set return temperature (black); Centre top: heating capacity (green), electrical power input (orange), mass flow rate (cyan); Centre bottom: temperature of mass H (red) and mass B (green), heat fluxes between heat pump and mass H (cyan), mass H and mass B (light grey), mass B and the ambient (purple); Bottom: outdoor temperature (green), relative humidity (grey).

HP2 shows defrost operation also at PLR B (Figure 12). The calculated building temperature decreases with each defrost but the temperature change is marginal. The reason is that lab 2 used the average supply temperature over period H (heating) instead of period H plus D (full cycle including defrost) to match the setpoint when adjusting the heating curve. It is considered to revise the test guideline accordingly (averaging period D+H) so that the building temperature can be used as control parameter which is supposed to remain constant for period H throughout the measurement.

Like for PLR A the return temperature oscillates around the setpoint during defrost. Despite the further reduced cooling load of the test stand the controllability does not improve. However, it is unlikely that the initially higher deviations affect the defrost process and the test stand brings

the return temperature very close to the setpoint rather fast. During the heating mode (period H) the deviation from the setpoint is only between 0.2-0.3 K.

PLR C

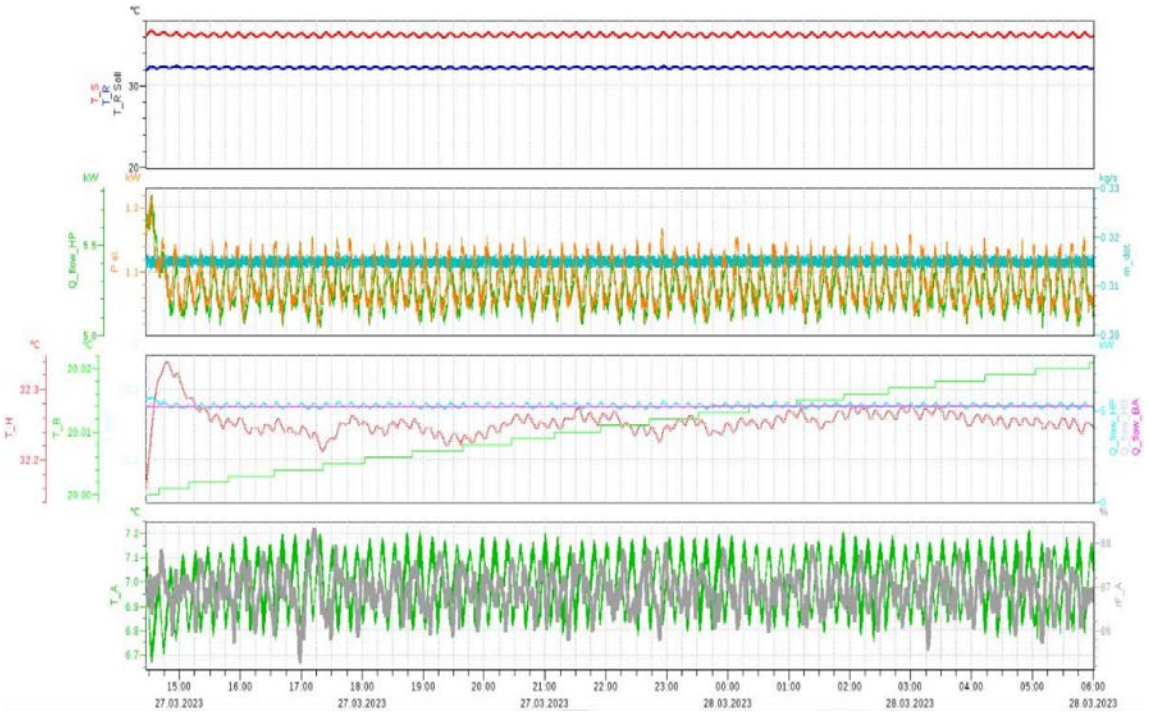

Figure 13: Time series of measured and calculated parameters at PLR C; Top: supply temperature (red), return temperature (blue), set return temperature (black); Centre top: heating capacity (green), electrical power input (orange), mass flow rate (cyan); Centre bottom: temperature of mass H (red) and mass B (green), heat fluxes between heat pump and mass H (cyan), mass H and mass B (light grey), mass B and the ambient (purple); Bottom: outdoor temperature (green), relative humidity (grey).

At PLR C the heat pump operates at constant compressor frequency without defrost operation due to the outdoor temperature of 7 °C (Figure 13). In contrast to HP3 the modulation limit is not reached yet for HP2 under the test conditions and the declared P_{design}. The supply and return temperatures oscillate in sinusoidal manner around the setpoint which is caused by interaction of the different controls. However, the deviation is rather low (about ±0.5 K).

PLR D

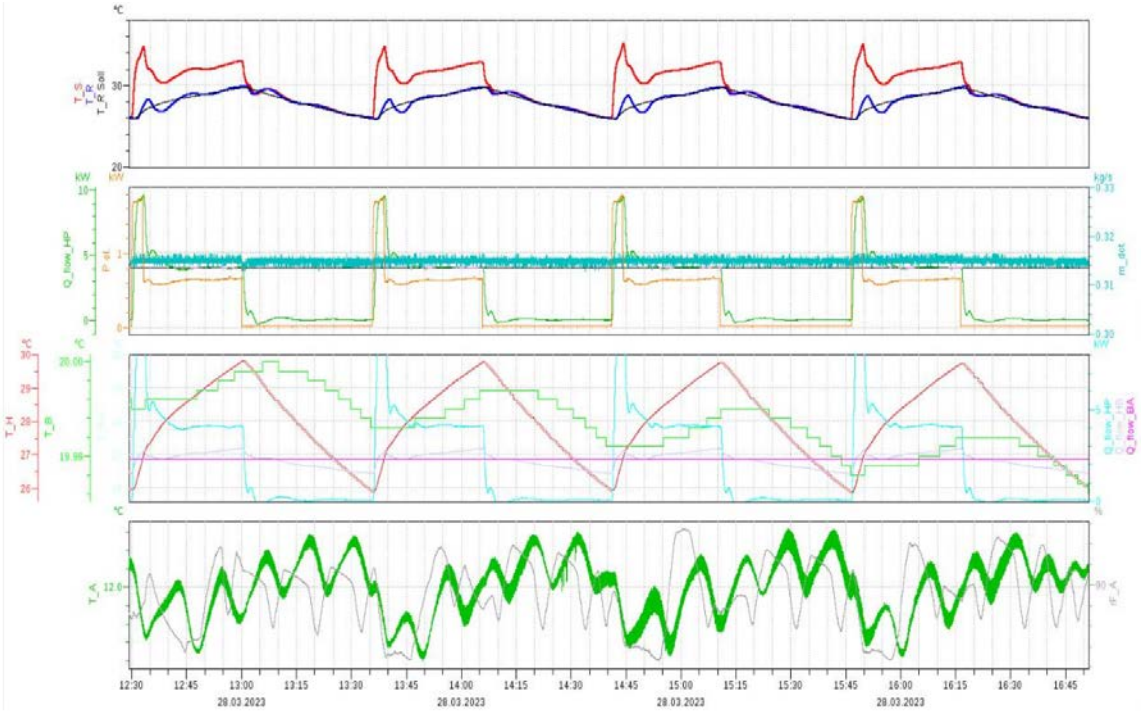

Figure 14: Time series of measured and calculated parameters at PLR D; Top: supply temperature (red), return temperature (blue), set return temperature (black); Centre top: heating capacity (green), electrical power input (orange), mass flow rate (cyan); Centre bottom: temperature of mass H (red) and mass B (green), heat fluxes between heat pump and mass H (cyan), mass H and mass B (light grey), mass B and the ambient (purple); Bottom: outdoor temperature (green), relative humidity (grey).

At PLR D the heat pump shows typical cyclic operation since the minimum compressor speed does not allow for steady state operation (Figure 14). The average supply temperature matches very well to the setpoint (29.7 °C instead of 30 °C). The deviation of the return temperature from the setpoint is very low except for the first 10 minutes after compressor start. However, those deviations are considered still acceptable with about ±1 K and for a limited period after compressor start. The operation behaviour of the unit is not expected to be influenced.

4.2.2. Including back-up heater

In addition to the measurements with deactivated electrical back-up heater, the operating behaviour was studied with active heater during the test. The reasoning has already been discussed in section 4.1.2. In the following it is shown that the heat pump controller of HP2 activates the back-up heater under test conditions E and A. This is in line with the previous observation that the bivalence temperature is higher than -7 °C for the declared P_{design} of 15 kW. At an outdoor temperature of 2 °C (test condition B) the heat pump can cover the load and the controller does not activate the back-up heater anymore. The measurements for PLR E and A are discussed in more detail below.

PLR E

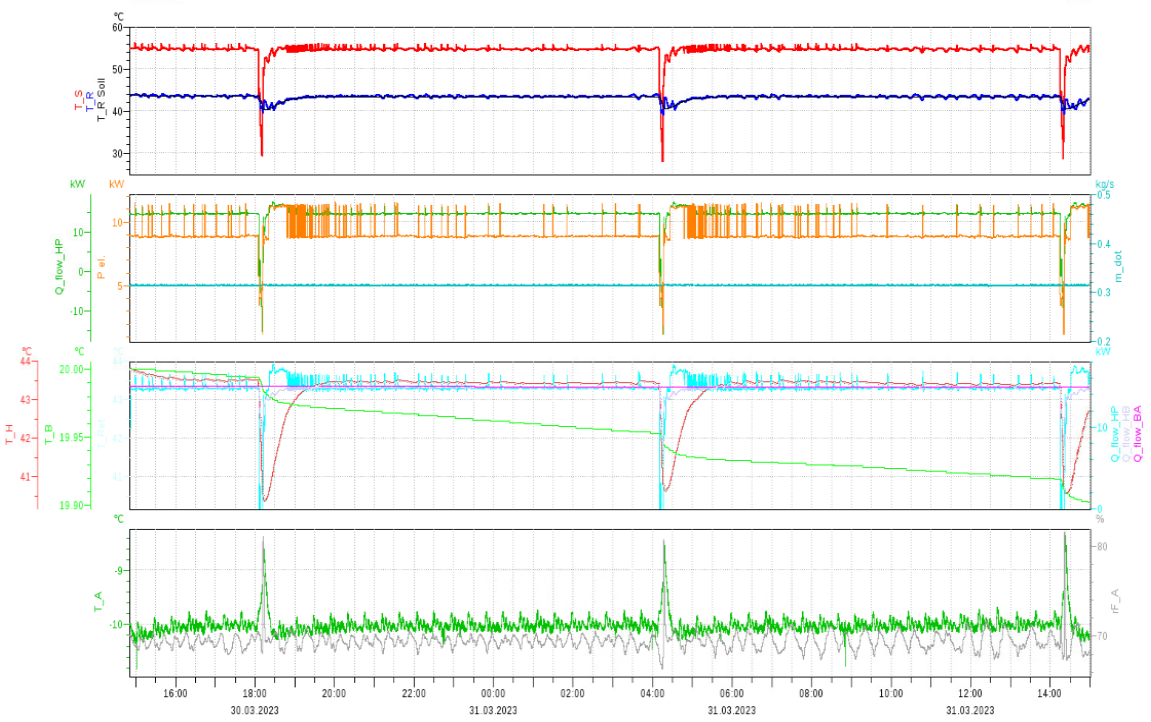

Figure 15: Time series of measured and calculated parameters at PLR E with active electrical back-up heater; Top: supply temperature (red), return temperature (blue), set return temperature (black); centre top: heating capacity (green), electrical power input (orange), mass flow rate (cyan); Centre bottom: temperature of mass H (red) and mass B (green), heat fluxes between heat pump and mass H (cyan), mass H and mass B (light grey), mass B and the ambient (purple); Bottom: outdoor temperature (green), relative humidity (grey).

Figure 15 show the operating behaviour of HP2 under test condition E with active electrical back-up heater. In contrast to the measurement without electrical back-up heater (Figure 10) the setpoints for the supply temperature and heating capacity are reached. From the spikes in the electrical power input it can be seen when the back-up heater starts to compensate for the deficit in the heat pump's heating power. Especially, after defrosting the back-up heater assists the heat pump in reaching the set supply temperature by higher switching frequency (18:45 and 04:45). When the supply temperature is stabilised, the frequency gradually decreases.

PLR A

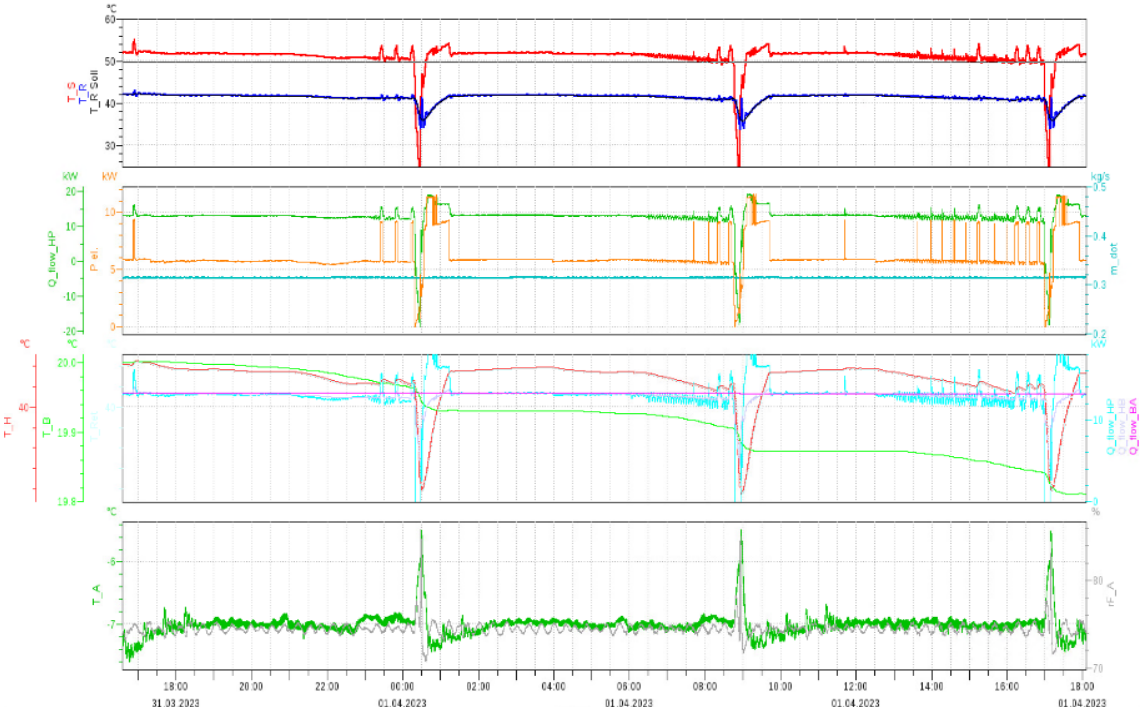

Figure 16: Time series of measured and calculated parameters at PLR A with active electrical back-up heater; Top: supply temperature (red), return temperature (blue), set return temperature (black); centre top: heating capacity (green), electrical power input (orange), mass flow rate (cyan); Centre bottom: temperature of mass H (red) and mass B (green), heat fluxes between heat pump and mass H (cyan), mass H and mass B (light grey), mass B and the ambient (purple); Bottom: outdoor temperature (green), relative humidity (grey).

Figure 16 shows the operating behaviour of HP2 with active back-up heater under test conditions A. As discussed previously the bivalence temperature is at a higher outdoor temperature than -7 °C (PLR A) for the declared Pdesign of 15 kW. Thus, the heat pump controller also activates the back-up heater under PLR A to reach the set supply temperature. Especially, after defrosting the heater assists in the recovery phase (e.g. 00:45) and before defrosting to compensate for icing of the evaporator (e.g. 13:30-17:00).

4.2.3. COPs and $SCOP_{on}$

Table 3 lists the COP and the mean values of different measured and calculated parameters for the five test conditions. The evaluation period is selected depending on the operating behaviour (defrost, continuous, on/off). For this study it was decided to evaluate a complete defrost cycle (period D + H) and four on/off cycles. The deviation between set and measured supply temperature could have been reduced for test conditions with defrosting (PLR E, A, B) because

the heating curve was adjusted to match the mean value of period H instead of period D+H to the set point.[5]

Table 3: Mean values calculated from the indicated evaluation period for the supply temperature, the emulated and the calculated return temperature, the measured heating capacity and electrical power input and the calculated COP for different test conditions. Assistance by the back-up (BU) heater is indicated for each test condition. For comparison COP_{bin} values measured according to EN 14511 are listed.

	PLR E	PLR A	PLR B	PLR C	PLR D
Condition	A-10W55	A-7W52	A2W42	A7W36	A12W30
Evaluation period	1 defrost cycle	1 defrost cycle	1 defrost cycle	70 min	4 on/off cycles
BU heater in use	yes	yes	no	no	no
ϑ_S [°C]	54.5	51.0	42.5	36.2	29.7
$\vartheta_{R,emu}$ [°C]	43.3	41.3	36.3	32.2	28.0
$\vartheta_{R,calc}$ [°C]	43.3	41.3	36.2	32.2	28.0
Q_{HP} [kW]	14.8	12.9	8.2	5.3	2.2
$P_{el,corr}$ [kW]	9.1	6.1	2.4	1.1	0.4
COP (Comp.)	1.6	2.1	3.4	4.8	6.0
COP_{bin} (EN 14511)	1.9	2.22	3.64	4.77	6.57
$SCOP_{on}$ (Comp.)			3.58		
$SCOP_{on}$ (EN14825)			3.70		

Only the measurements with active electrical back-up heater are used for the COP calculation. Therefore, the measured heating capacity and electrical input power already include the share of the back-up heater and no further correction is required. PLR F was not measured and the $SCOP_{on}$ is calculated only from the COPs for the five measured test points despite the observation that $T_{biv} > -7$ °C for the declared P_{design} as discussed before. Based on the COPs in Table 3 the $SCOP_{on}$ is equal to 3.58.

Table 3 lists also COPs measured on HP2 according to EN 14511 kindly provided by the manufacturer.[6] As discussed before, for test conditions where the setpoint of the heating capacity in EN 14511 tests is not reached the COP difference between both methods cannot be compared directly (section 4.1.3). For HP2 this applies only to PLR E for which the highest deviation is observed. For PLR A the difference is rather small and for PLR B slightly higher. The deviation might be explained similar as for HP1 with differences in capturing the defrost and the imperfect[7] operation of the back-up heater (compare section 4.1.3). At the lowest part load (PLR D) the offset is -10 % which is inline with observations in previous work. [3] It is assumed that the difference is due to losses during on/off operation which are not accurately taken into

5 In principle, the permissible deviation of ±0.3 K according to EN 14511 is too tight since the heating curve of many heat pumps can only be adjusted by 1 K increments. Sticking to the permissible deviations of the standard would force manufacturers to adapt the heat pumps' controls and sensors.

6 It should be noted that after the compensation measurements and before the EN 14511 tests the heat pump controller was optimized by the manufacturer which may have led to improved results in the EN 14511 tests.

7 Compared to other heat pumps the three-staged back-up heater is well operated in the tests.

account by the degradation factor applied in the standard test to correct the data for cycling. Compared to HP1, the offset is much smaller for PLR D, indicating that the offset and losses due to on/off operation are individually dependent on the heat pump, presumably on its control. The finding underlines the need to test also the heat pump control to ensure comparability between appliances and create a level playing field.

The $SCOP_{on}$ according to EN 14825 calculates to 3.70 and is about 3 % higher than the one calculated from the compensation data. This result illustrates again that good heat pumps are not rated much worse compared to the current standard. However, poor performing controls will be rated lower. Thus the compensation method allows for a more representative rating of products.

4.3. Lab 3 – ILK

Lab 3 performed measurements with fixed flow (section 4.3.1) and variable flow settings (section 4.3.2). Those measurements were performed using the heating curve of the heat pump to achieve the supply temperature setpoints. In addition, the interaction of the building model with the indoor temperature control of the heat pump was assessed in separate tests (section 4.3.3). For all measurements the P_{design} of 6.5 kW declared by the manufacturer for medium temperature application and average climate was used to calculate the part load capacities.

4.3.1. Heating curve and fixed flow

The first measurements in lab 3 were performed with a fixed flow setting of 10.3 l/min. In the following paragraphs, the operation behaviour of the heat pump under the selected test conditions is discussed.

PLR E

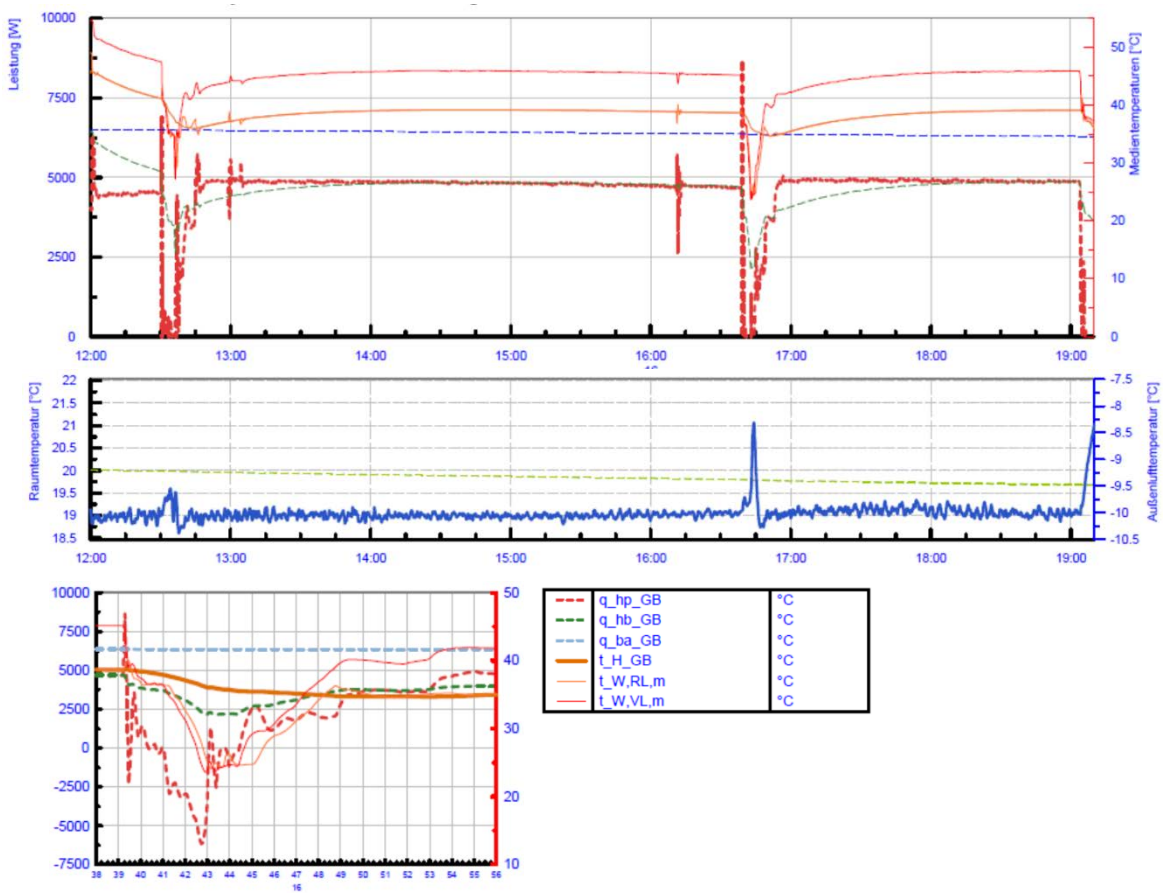

Figure 17: Time series at PLR E for measured and calculated parameters; Top: supply temperature (t_W,VL,m), return temperature (t_W,RL,m), heating capacity (q_hp_GB), calculated heat fluxes between mass H and B (q_hb_GB) and mass B and the ambient (q_ba_GB), calculated set return temperature (t_H_GB); Centre: calculated building temperature (green), measured outdoor temperature in the climate chamber (blue); Bottom: magnified view of the defrost cycle at about 16:00.

The time series of the measured supply and return temperatures are shown in Figure 17 along with the heat fluxes and temperatures calculated by the building model for PLR E. At 12:00 the building model was activated on the test stand control leading to a decrease in heating capacity and supply temperature of the heat pump due to a change in load conditions compared to the initial starting conditions not shown (before 12:00). The return temperature setpoint and the heat flux between mass H and B calculated by the building model decrease accordingly. At 12:30 the heat pump controller initiates a defrost cycle which lasts for about four hours (period D plus H according to EN 14511). The second defrost cycle is much shorter (about 2.5 hours). Differences in the length of the first and second defrost cycle are commonly observed

for A/W heat pumps according to test institutes, which might be incentivised by the prescriptions of EN 14511 on defrost evaluation.[8]

The lower graph of Figure 17 shows a magnified inset of the second defrost cycle at about 16:30. It can be observed that the return temperature drops below the set point calculated by the building model. This issue is related to the optimisation of the control parameters of the test stand's mixing valve and could be solved by adding an electrical heater in front of the return to the heat pump. This solution was applied for the variable flow measurements (section 4.3.2). The test stand modifications and a comparison of defrost measurements before and after are discussed in more detail in section 3.2.

In general, the heat pump shows typical operation behaviour for an A/W heat pump at full load conditions. However, the average supply temperature is too low compared to the set point (45.3 °C instead of 55 °C) and the calculated building temperature constantly decreases, indicating that the heat pump cannot achieve the required heating capacity without the electrical back-up heater being activated. This is common since manufacturers are free to optimise the SCOP by choosing the bivalence point. Nevertheless, the declared P_{design} seems to be too high as will be discussed in more detail for the lower part load conditions. It has been discussed in section 4 that the (virtual or real) back-up heater must be active during the test. Including the back-up heater in the test was, however, only tested by lab 1 and lab 2.

[8] According to the current standard the temperature difference between supply and return temperature (5 minute average) is compared at the beginning of period H and after 70 min. If the deviation is below 2.5 % the measurement is stopped and no defrost is considered. Therefore, it can be beneficial for performance evaluation according to EN 14511 to extend the heating period (period H) by delaying defrosting (period D) despite decreasing heating capacity due to icing. This issue is not directly related to the compensation method but has been addressed in the latest test guideline published by BAM and will be discussed in CEN/TC 113/WG 8 and on regulatory level.

PLR A

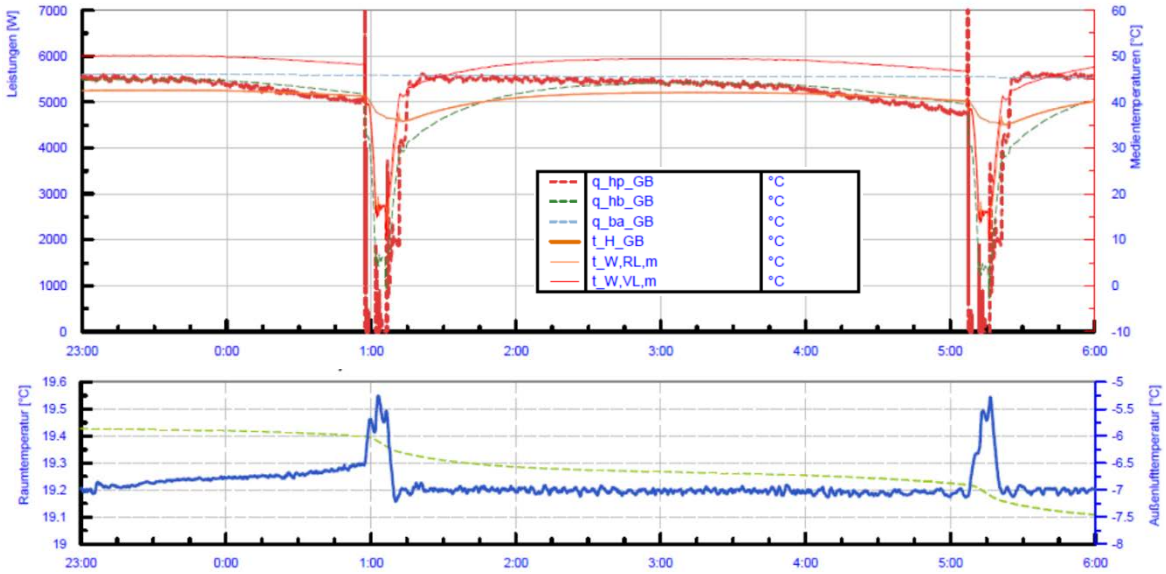

Figure 18: Time series at PLR A for measured and calculated parameters; Top: supply temperature (t_W,VL,m), return temperature (t_W,RL,m), heating capacity (q_hp_GB), calculated heat fluxes between mass H and B (q_hb_GB) and mass B and the ambient (q_ba_GB), calculated set return temperature (t_H_GB); Bottom: calculated building temperature (green), measured outdoor temperature in the climate chamber (blue).

Figure 18 shows the time series of the measured supply and return temperatures as well as the heat fluxes and temperatures calculated by the building model for PLR A. The graph shows only the evaluated defrost cycle (data between 1:00 and about 5:00). In total five complete defrost cycles were recorded which were very reproducible in length and temperature levels. Similar to the observations for PLR E the supply temperature is too low compared to the set point (48.4 °C instead of 52 °C) and the building temperature decreases with each defrost (period D) and even during on-phases off the compressor (period H). This indicates a too low heating capacity resulting from a too high declared P_{design}. During defrost operation the test stand cannot follow the return temperature setpoint which was discussed already for PLR E. Overall the heat pump shows typical operation behaviour indicating that the two-mass building model works as expected.

PLR B

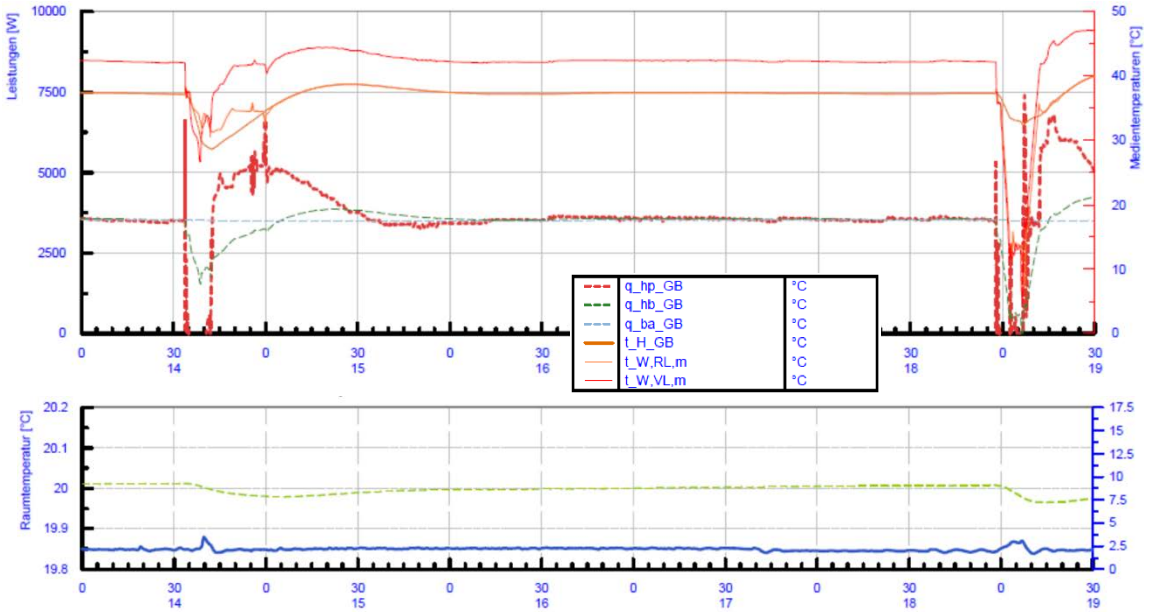

Figure 19: Time series at PLR B for measured and calculated parameters; Top: supply temperature (t_W,VL,m), return temperature (t_W,RL,m), heating capacity (q_hp_GB), calculated heat fluxes between mass H and B (q_hb_GB) and mass B and the ambient (q_ba_GB), calculated set return temperature (t_H_GB); Bottom: calculated building temperature (green), measured outdoor temperature in the climate chamber (blue).

Figure 19 shows the time series for PLR B of the measured and calculated temperatures and heat fluxes. The heat pump operates still in defrost operation as expected for these test conditions. In contrast to PLR E and PLR A the supply temperature averaged over the full defrost cycle (period H and D) matches very well the set point (42.5 °C instead of 42 °C). Considering the accuracy of common heat pump controllers, the observed deviation of +0.5 K is considered acceptable and within the permissible deviations of ±1 K proposed in the revised test guideline. Thus, the heat pump can achieve the required heating capacity at PLR B without back-up of the electrical heater and the building temperature is constant (only minor deviations are observed during defrosting).

Based on the previous observation (PLR E and PLR A) that the test stand cannot follow the set point of the return temperature during defrost, lab 3 installed an electrical heater in the water loop of the test stand. In a first attempt the heater was controlled manually by the staff. As can be seen during the first defrost around 14:30 in Figure 19 the return temperature does not drop below the setpoint anymore. However, the return temperature level is now too high and the manual controllability limited. Therefore, the lab did not use the electrical heater during the second defrost at 19:00, as long as no automatic control was implemented.[9]

[9] Meanwhile the electrical heat has been implemented with automatic control in lab 3 showing good controllability of the return temperature.

PLR C

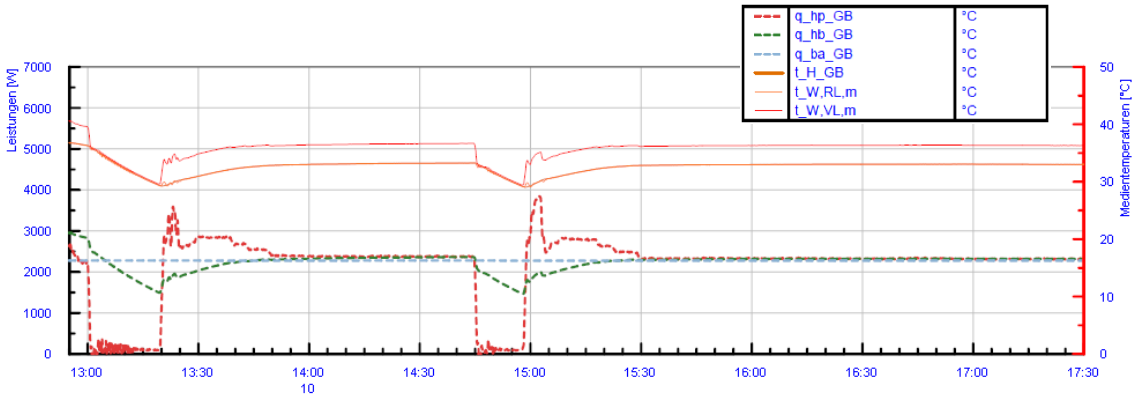

Figure 20: Time series at PLR C for measured and calculated parameters; supply temperature (t_W,VL,m), return temperature (t_W,RL,m), heating capacity (q_hp_GB), calculated heat fluxes between mass H and B (q_hb_GB) and mass B and the ambient (q_ba_GB), calculated set return temperature (t_H_GB).

PLR C is rather close to the modulation limit of inverter driven compressors. Therefore, on-off operation may or may not occur depending on the specific minimum compressor frequency (modulation limit) of the unit under test.

The time series of the measurements for PLR C are depicted in Figure 20. At about 13:00 the compressor of the tested heat pump turns off and restarts about 20 min later. Another on-off cycle starts at about 14:45. For the remaining measurement time (2.5 h) the compressor runs almost steady state and no further on-off cycle is observed. Since the measurement was stopped it is unclear whether on-off cycling continues or not. Nevertheless, comparing the duration of the first and second (uncomplete) cycle it is apparent that the on-phases of the two cycles differ at least by 30 min. From the recorded data it cannot be concluded if alternating cycle length occur or the unit would continue in steady-state operation.

It is possible that the compressor frequency is at a tipping point (modulation limit) causing inconsistent operation behaviour. However, this can be changed by lowering the (too high) P_{design} because the part-load capacities are calculated from the design capacity.[10] In general, this observation is not considered problematic since manufacturers have an incentive to ensure reproducible measurements (by carefully choosing the P_{design}) in case of market surveillance.

The feasibility of the compensation method is not questioned but it might be necessary to include further prescriptions in the test guideline to ensure reproducible results in different labs. In that respect, the planned round robin test could contribute further valuable data and information on the operation behaviour in different labs and possible measures. It could be assessed whether longer test times and evaluation periods should be foreseen to level-out differences in operation

[10] In the ongoing round robin test (38943/01) this issue is solved by lowering the P_{design} until PLR A becomes the bivalence point moving also PLR C away from the compressor frequency limit.

behaviour in different labs, for example. The Canadian draft standard CSA SPE07:2023 for load-based testing of air-to-air air conditioners uses a conversion criterion, for instance, which might be possible to adapt to the compensation method.

PLR D

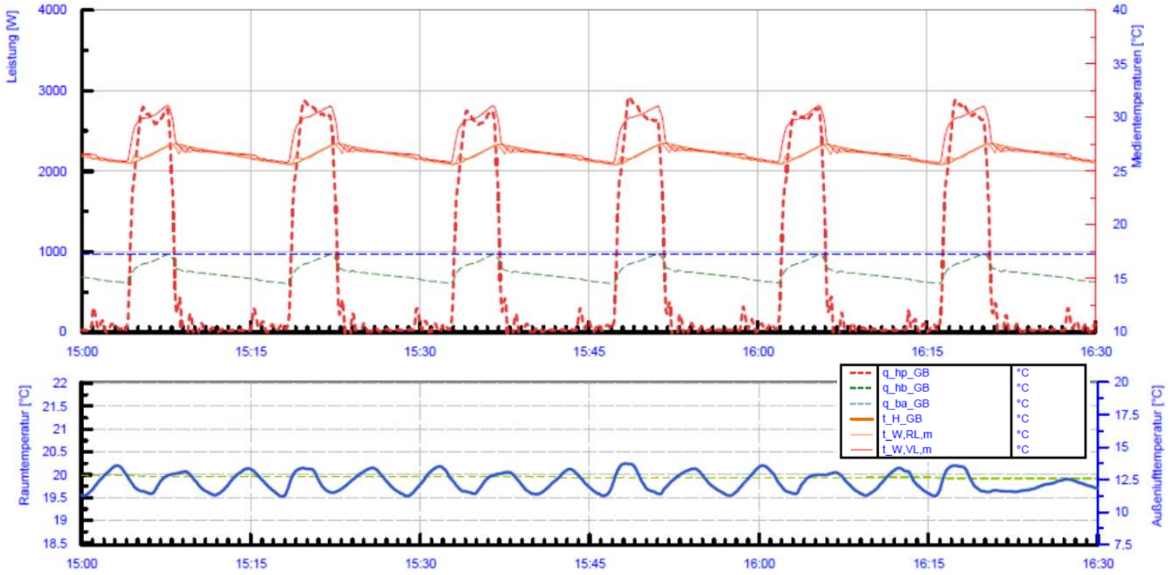

Figure 21: Time series at PLR D for measured and calculated parameters; Top: supply temperature (t_W,VL,m), return temperature (t_W,RL,m), heating capacity (q_hp_GB), calculated heat fluxes between mass H and B (q_hb_GB) and mass B and the ambient (q_ba_GB), calculated set return temperature (t_H_GB); Bottom: calculated building temperature (green), measured outdoor temperature in the climate chamber (blue).

Figure 21 shows the operation behaviour of the heat pump under test condition D. The part-load capacity for this test point is so low that the compressor of the heat pump is at its frequency limit resulting in on-off operation of the compressor. The average supply temperature is too low (26 °C instead of 30 °C) since the set point of the heating curve refers to compressor-on periods only, not the average value over full cycles.[11] In this case the heating curve shall be adjusted according to the test guideline. It is expected that the heat pump would increase the temperature level during on-phases after adjusting the heating curve[12], even though it was read from the display that the unit operates with minimum on and off-times of the compressor. However, lab 3 did not adjust the heating curve due to time constrains. For the proof-of-concept this deviation from the prescribed test condition is not an issue since realistic interaction between heat pump and tests rig is shown also under very low part-load conditions. Furthermore, the test stand is capable to

[11] From experience it is manufacturer dependent whether the heat pump controls the supply temperature on the average value of full cycles (anticipating off-times) or solely on on-periods of the compressor.
[12] The assumption has been confirmed in preparation of the round robin test. The average supply temperature can be reached by adjusting the heating curve.

follow the calculated return temperature set point quite well even under the dynamics of frequent cyclic operation.

4.3.2. Heating curve and variable flow

HP3 was tested also with variable flow settings of the controller. The temperature spread over the condenser was set to 8 K. During the measurements the sink side volume flow was controlled only by the heat pump and realised by the internal circulation pump. To calculate the part-load capacities the same P_{design} of 6.5 kW was used as for the measurements with fixed flow.

PLR B

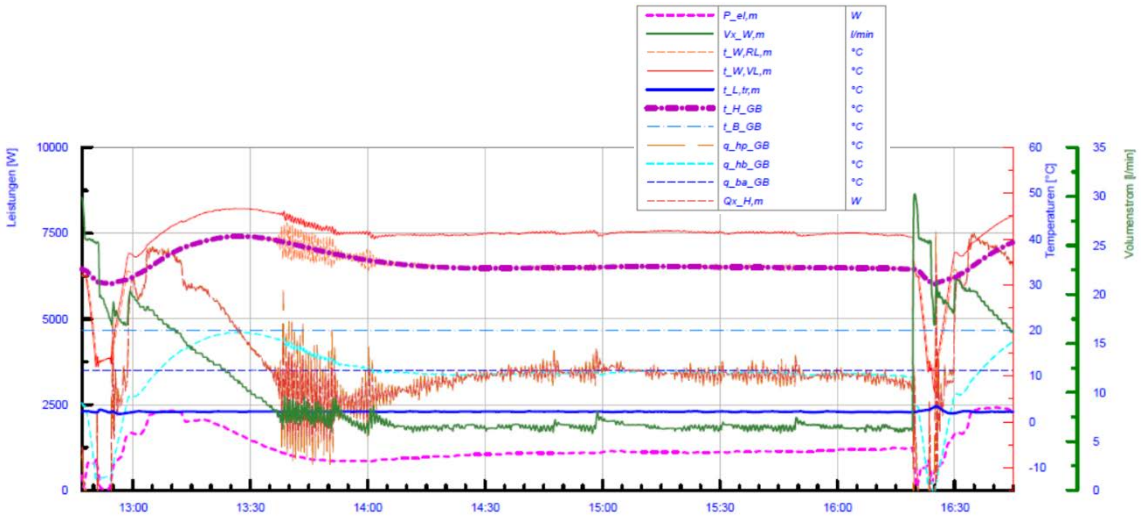

Figure 22: Time series at PLR B (variable flow) for the measured and calculated parameters; heating capacity (q_hp_GB), calculated heat fluxes between mass H and B (q_hb_GB) and mass B and the ambient (q_ba_GB), calculated set return temperature (t_H_GB), calculated building temperature (t_B_GB), supply temperature (t_W,VL,m), return temperature (t_W,RL,m), outdoor air temperature in the climate chamber (t_L,tr,m), flow rate (Vx_W,m), electrical power input (P_el,m).

Figure 22 shows the operation behaviour of the HP3 under test condition B with variable flow control. As for fixed flow the unit defrosts. However, the cycle length with variable flow is about one hour shorter. With defrost start the heat pump instantaneously increases the flow rate probably to increase the heat transfer and minimise the deficit in heating power. When the compressor restarts the flow is slowly reduced again until it stays almost constant at a rather low level.

As for the fixed flow measurements, during defrost operation the return temperature cannot follow the calculated set point because no electrical heater was installed yet in the return to the heat pump. Between 13:40 and 14:05 oscillation of the flow rate, the supply and return temperature is observed leading to high deviations from the calculated return temperature set point. The reason is still analysed but similar behaviour is known from hard-ware in-the-loop (HiL)

tests at RWTH when domestic hot water tapping is emulated requiring very low flow rates. From experience this issue can be solved by flow dependent PID settings of the mixing valve controller to slow down the valve response at low flow rates.[13]

In summary the heat pump shows realistic operation behaviour even though the test rig control settings can be improved. Thus, variable flow units can be tested even under the dynamics of defrost operation.

PLR D

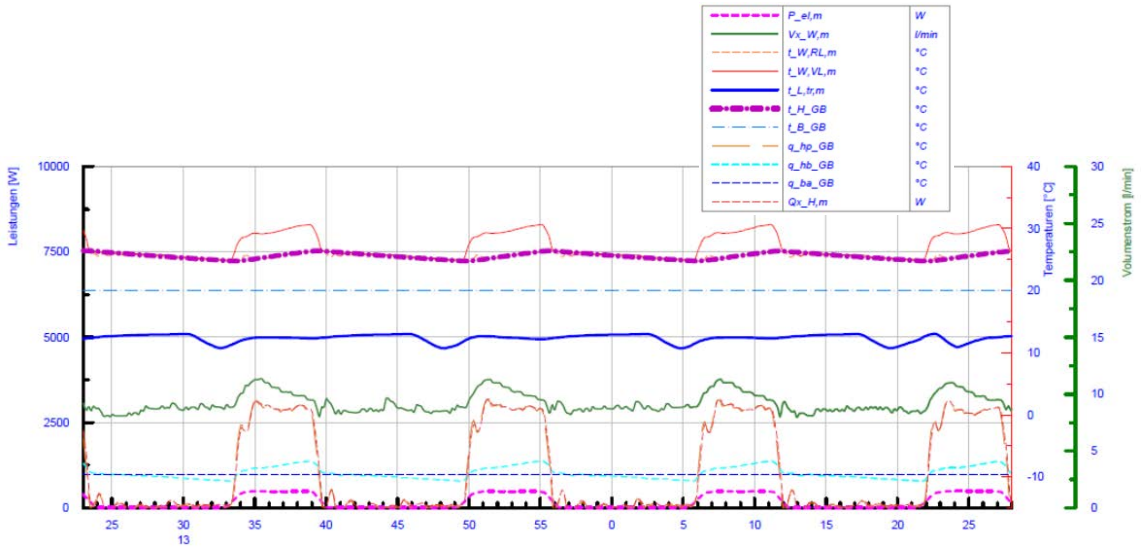

Figure 23: Time series at PLR D (variable flow) for the measured and calculated parameters; heating capacity (q_hp_GB), calculated heat fluxes between mass H and B (q_hb_GB) and mass B and the ambient (q_ba_GB), calculated set return temperature (t_H_GB), calculated building temperature (t_B_GB), supply temperature (t_W,VL,m), return temperature (t_W,RL,m), outdoor air temperature in the climate chamber (t_L,tr,m), flow rate (Vx_W,m), electrical power input (P_el,m).

Figure 23 shows the heat pump operation under test condition D. The compressor cycles on-off because the minimum compressor speed is too high to cover the low load. The cycle patterns (on/off times) are very similar compared to the fixed flow setting but the heat pump slightly increases the flow during on-periods. The average supply temperature is too low again and the heating curve must be adjusted.

Also, under the dynamics of cyclic operation the test stand controls the return temperature closely to the setpoint. It is concluded that also for test condition D the interaction of the test stand and the heat pump works properly and realistic operation is observed.

[13] It is planned to verify the hypothesis with HP3 at RWTH in the context of the planned round robin test.

4.3.3. Indoor temperature control

According to manufacturers heat pumps are expected to be placed on the market that are designed for very well insulated houses and are controlled on the indoor air temperature only (not the outdoor air temperature). Those products can only be tested by emulating the indoor air temperature by means of a building model. To the knowledge of the authors the vast majority of heat pumps still have a heating curve (at least optional). Therefore, including the indoor air temperature control in the test is considered optional for the time being and not a requirement for introducing the compensation method. Nevertheless, it was decided to assess the feasibility of the concept in this study.

The building model developed by the project partners is designed to be as simple as possible while being as accurate as necessary. However, pretest have shown very slow response of the building temperature calculated by the two-mass model which is used to emulate the indoor air temperature. Therefore, it might be necessary to extend the two-mass model to describe the heat transfer between the heating system (emitters) and the indoor air more realistically. The modification is expected to be rather simple and will be assessed in further studies. For this proof-of-concept internal gains and losses (e.g. solar gains or open windows) were introduced to accelerate the change in building temperature.

Lab 3 performed tests on HP3 to assess the interplay between the test stand and the heat pump using a mix of indoor and outdoor air (heating curve) temperature control. The indoor temperature could be emulated successfully by placing the thermostat in a climate box. It was shown that the heat pump responds to changing internal gains and losses by adjusting the heating capacity, as expected. Thus, the feasibility could be demonstrated as discussed below.

PLR B

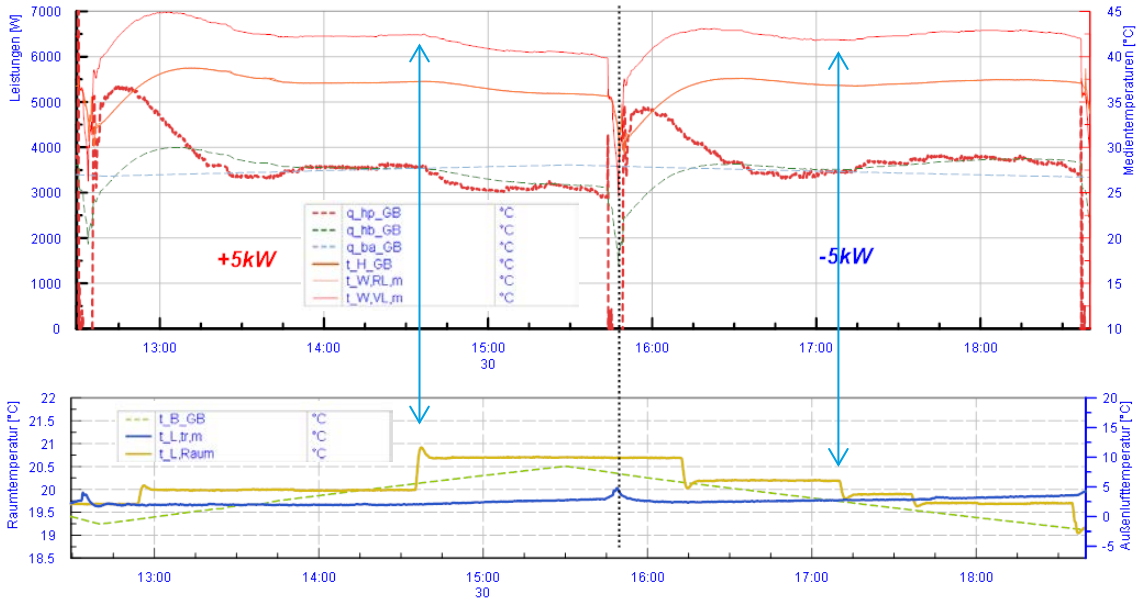

Figure 24: Influence of internal gains and losses on the operating behaviour at PLR B; Top: supply temperature (t_W,VL,m), return temperature (t_W,RL,m), calculated set return temperature (t_H_GB), heating capacity (q_hp_GB), calculated heat fluxes between mass H and B (q_hb_GB) and mass B and the ambient (q_ba_GB); Bottom: calculated building temperature (t_B_GB), measured outdoor temperature in the climate chamber (t_L,tr,m), manually controlled climate box temperature (t_L_Raum)).

To demonstrate the response of the heat pump controller on a changing indoor temperature the building model was modified to simulate constant internal gains or losses in order to accelerate the temperature change and shorten the test time. The heat pump's temperature sensor was placed in a climate box whose temperature was manually changed to follow the calculated building temperature. The manual control was done in steps of 0.75 K corresponding to the increment of the displayed room temperature on the heat pump's controller.

Figure 24 shows measured and calculated temperature und heat fluxes under test condition B. At 12:45 an internal gain of +5 kW is simulated and the building temperature (lower graph) linearly increases. At 15:30 an internal loss of -5 kW is simulated and the building temperature linearly decreases. The increase/decrease in building temperature is followed by increasing/decreasing the climate box's temperature in discrete steps. While the response of the heat pump controller on the first temperature increase at 12:55 is overlayed by the supply temperature increase after defrost (recovery phase) the second increase at 16:15 triggers the heat pump controller to reduce the supply temperature (left arrow). This becomes more obvious when comparing the first defrost cycle (+5 kW gain) to the second cycle (-5 kW loss). In contrast to the first defrost cycle the temperature decrease at 17:15 (right arrow) triggers the controller to increase of the supply temperature.

PLR C

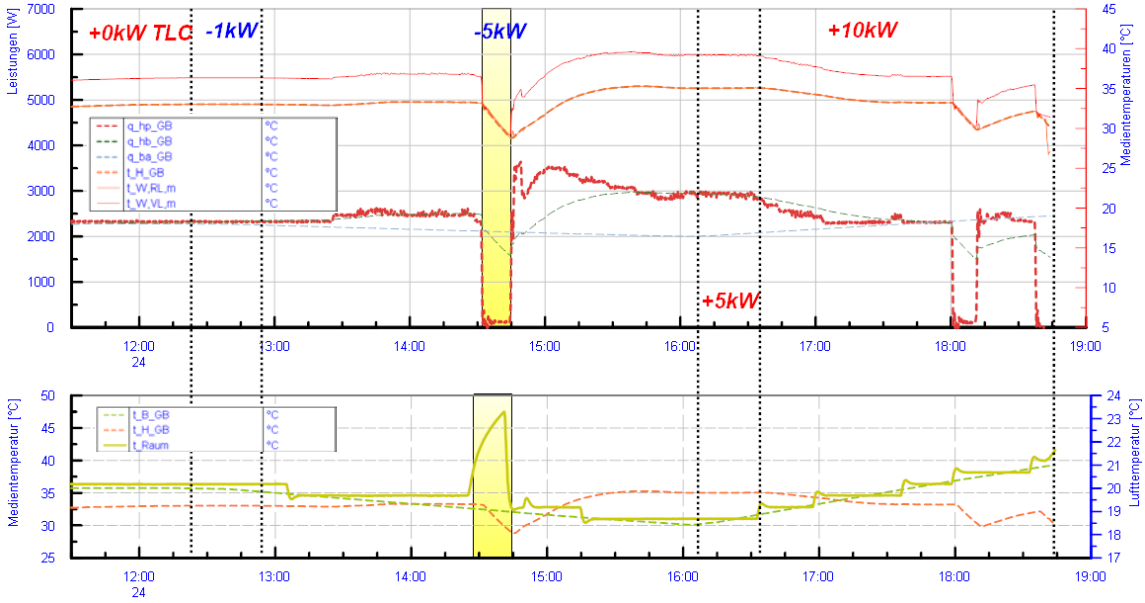

Figure 25: Influence of internal gains and losses on the operating behaviour at PLR C; Top: supply temperature (t_W,VL,m), return temperature (t_W,RL,m), calculated set return temperature (t_H_GB), heating capacity (q_hp_GB), calculated heat fluxes between mass H and B (q_hb_GB) and mass B and the ambient (q_ba_GB); Bottom: calculated building temperature (t_B_GB), measured outdoor temperature in the climate chamber (t_L,tr,m), manually controlled climate box temperature (t_L_Raum)).

Figure 25 shows the measured and calculated temperatures and heat fluxes at PLR C. As discussed previously the heat pump is close to the modulation limit of the compressor at PLR C for the declared P_{design} of 6.5 kW. The measurement starts with continuous operation. At 12:20 a loss of -1 kW is set in the script and the calculated building temperature decreases slightly. At 13:10 the climate box temperature was decreased manually by 0.75 K to follow the building temperature. The heat pump controller responds with a delay of about 20 minutes at 13:30 by increasing the supply temperature slightly. At 14:30 the climate box shuts off due to an error and the temperature in the box quickly increases. This triggers the heat pump controller to shut off the compressor until it is restarted at 14:45 because the climate box temperature is decreased again to follow the calculated set point. Due to the further decreasing building (climate box) temperature the supply temperature level is about 2.5 K higher after the restart compared to before.

At 16:10 internal gains are simulated. The supply temperature is gradually decreased by the controller starting from the first increase in climate box temperature at 16:35. At 18:00 the unit goes in on/off operation (modulation limit) to reduce the heating capacity further.

PLR D

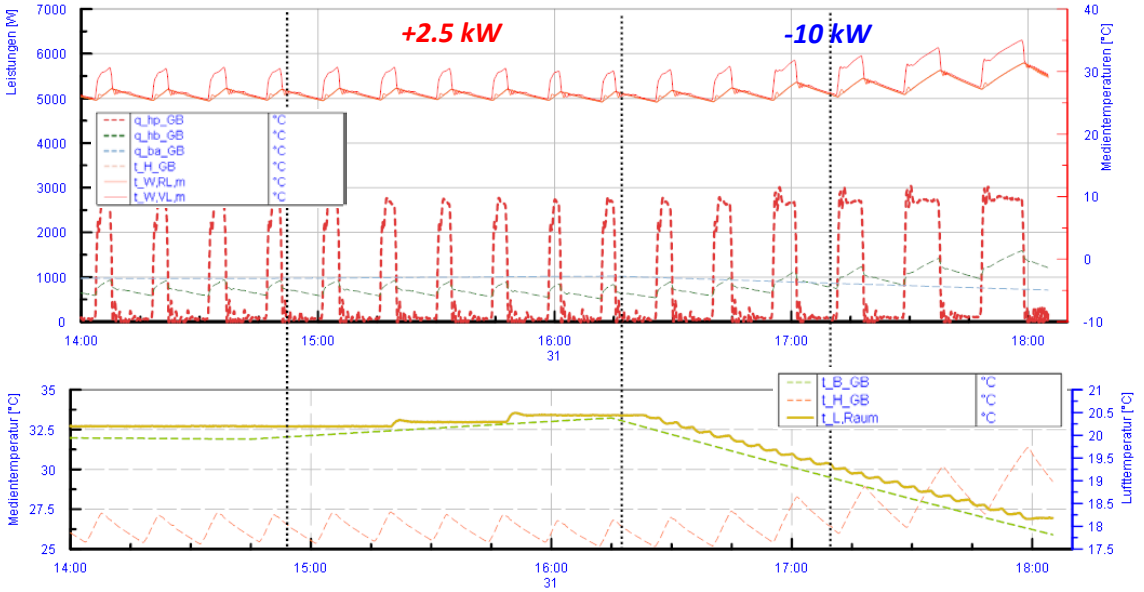

Figure 26: Influence of internal gains and losses on the operating behaviour at PLR D; Top: supply temperature (t_W,VL,m), return temperature (t_W,RL,m), calculated set return temperature (t_H_GB), heating capacity (q_hp_GB), calculated heat fluxes between mass H and B (q_hb_GB) and mass B and the ambient (q_ba_GB); Bottom: calculated building temperature (t_B_GB), measured outdoor temperature in the climate chamber (t_L,tr,m), manually controlled climate box temperature (t_L_Raum)).

Figure 26 shows the measured and calculated temperatures and heat fluxes at PLR D. The heat pump's compressor runs in on/off operation. At about 14:55 an internal gain of 2.5 kW is simulated which causes the building temperature to increase. The climate box temperature is manually increased at 15:20 and 15:50 to emulate the building temperature increase. The heat pump controller does not react to the first increase but to the second step by slightly lowering the on-cycle temperature level. At 16:15 a loss of -10 kW is simulated. Consequently, the controller gradually increases the supply temperature level during the on-phases and increases the on-phase duration to compensate the loss.

5. Sensitivity analysis

The sensitivity analysis examines the influence of deviations between the return temperature controlled by the test bench and the set temperature specified by the two-mass model on the test result (COP). For this purpose, four tests were performed emulating different faults. In two tests, the return temperature was manipulated by a constant value of +1 K and -1 K, respectively. In two other tests, a possible oscillation (similar to the ones observed in lab 2) due to limited controllability was emulated. A deviation from the set return temperature was determined by a sinusoidal function, which has an amplitude of 1 K and 2 K, respectively. From the results permissible deviations for the revised test guideline are derived.

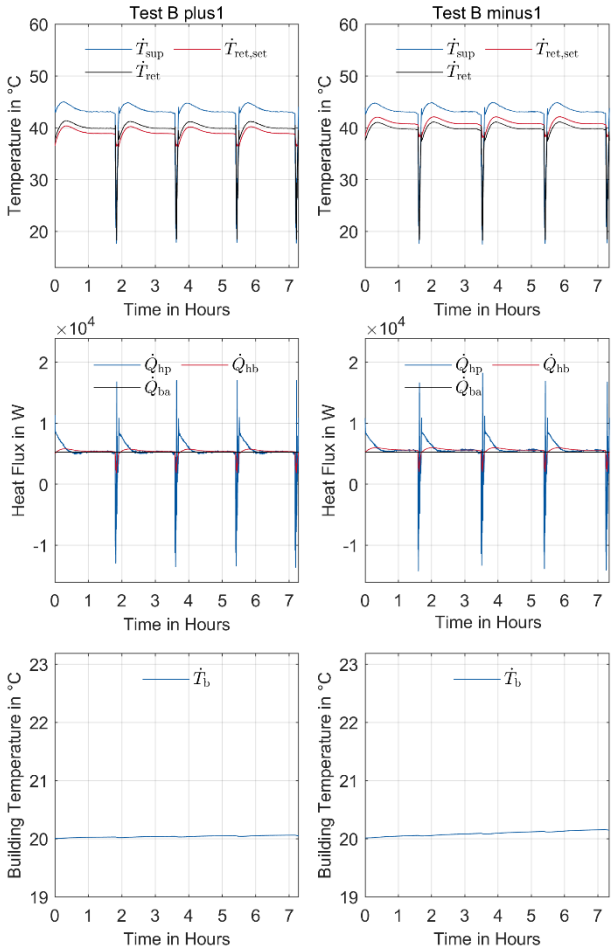

Figure 27: Heat pump operation with the two-mass model for test points B with manipulated return temperature, +1 K (left-hand side), -1 K (right-hand side); Top: supply temperature ϑ_s (here: T_{sup}), return temperature $\vartheta_{R,emu}$ (here: T_{ret}), and return set temperature $\vartheta_{R,calc}$ (here: $T_{ret,set}$); Center: heat flow from heat pump into mass H $\dot{Q}_{HP}$, heat flow from mass H into mass B $\dot{Q}_{HB}$, heat flow from mass B into the environment $\dot{Q}_{BA}$; Bottom: temperature of virtual building $\vartheta_{B,calc}$ (here: T_b).

Figure 27 shows the results of the first two tests. The intentionally introduced offset can be seen when comparing the return temperature $\vartheta_{\mathrm{R,emu}}$ (black line), and the return set temperature $\vartheta_{\mathrm{R,calc}}$ (red line). Both faults have no impact on the heat pump's operating behaviour.

Furthermore, the return temperature $\vartheta_{\mathrm{R,emu}}$ is on the same temperature level for both emulated faults (+1 K / -1 K). Figure 29 shows the average temperatures of all four tests with emulated faults compared to one test without faults for test point B. Comparing Test B, Test B plus 1 and Test B minus 1 it can be observed that the average supply temperature (blue bar) and the average return temperature (green bar) are in all three tests identical. This shows that the constant faults do not influence the heat pump operation in tests with the two-mass model. The two-mass model compensates for the error by adjusting the setpoint for the return temperature. For simplification, the dynamic process is described step by step and exemplarily for Test B plus 1:

1. The manipulation leads to a higher return temperature while the heat pump keeps the supply temperature constant which leads to a decreased heating capacity.
2. The smaller heating capacity of the heat pump $\dot{Q}_{\mathrm{HP}}$ results in a decreasing temperature of mass H in the two-mass model ($\vartheta_{\mathrm{R,calc}}$) since the heat flow from mass H into the building $\dot{Q}_{\mathrm{HB}}$ is almost constant. The following equation describes the temperature change over time:
$$\frac{d\vartheta_{\mathrm{R,calc}}}{dt} = \frac{\dot{Q}_{\mathrm{HP}} - \dot{Q}_{\mathrm{HB}}}{C_{\mathrm{H}}}$$
3. The temperature of mass H provides the return set temperature for the test, thus the return set temperature decreases until the heat flow $\dot{Q}_{\mathrm{HP}}$ and the heat flow $\dot{Q}_{\mathrm{HB}}$ are equal.

The analysis of the constant offsets shows that the deviation does not influence the heat pump behavior and the energetic results. Nevertheless, constant deviations are rarer than oscillations due to bad controller settings. For this reason, controller errors are emulated by sinusoidal deviations of the return temperature. The results are shown in Figure 28. The average values are not significantly affected since the positive and negative deviations are in the same range. Nevertheless, Figure 29 underlines that sinusoidal deviations of 2 K affect the heat pump operation. The supply temperature decreases from 43.8 °C (Test B) to 43.3 °C (Test B sinus plus 2). Presumably, the heat pump controller reacts to the oscillations, influencing the energetic values. While the constant fault deviations lead to efficiency (COP) changes in a two percent range which is still within the measurement uncertainty, the sinusoidal deviation influences the efficiency by 3.5 % and 9.7 % for 1 K amplitude and 2 K amplitude, respectively. Therefore, oscillations higher than 1 K should be avoided or restricted to periods where operation behaviour is certainly not affected (e.g. for short periods after compressor start).

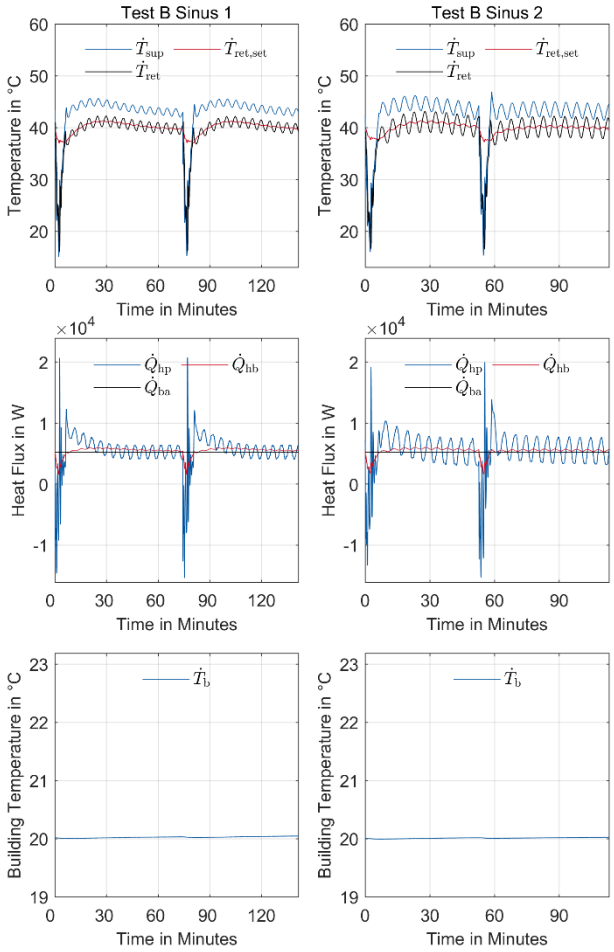

Figure 28: Heat pump operation with the two-mass model for test points B with sinusoidal manipulated return temperature, amplitude +1 K (right-hand side), amplitude +2 K (left-hand side); Top: supply temperature ϑ_s (here: T_{sup}), return temperature $\vartheta_{R,emu}$ (here: T_{ret}), and return set temperature $\vartheta_{R,calc}$ (here: $T_{ret,set}$); Center: heat flow from heat pump into mass H $\dot{Q}_{HP}$, heat flow from mass H into mass B $\dot{Q}_{HB}$, heat flow from mass B into the environment $\dot{Q}_{BA}$; Bottom: temperature of virtual building $\vartheta_{B,calc}$ (here: T_b).

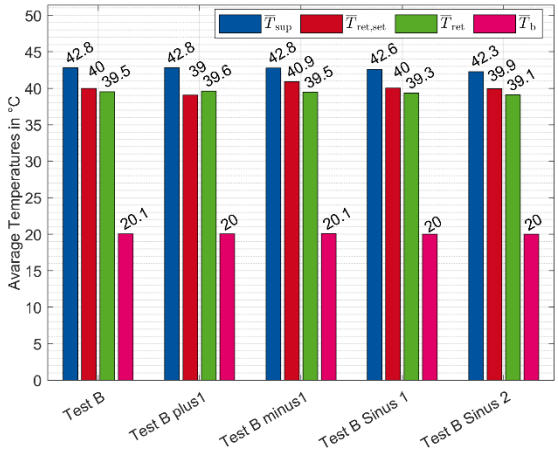

Figure 29: Average supply temperature ϑ_s (here: T_{sup}), return temperature $\vartheta_{R,emu}$ (here: T_{ret}), return set temperature $\vartheta_{R,calc}$ (here: $T_{ret,set}$), and building temperature under test conditions B for the correct test, constant return temperature deviation, and sinusoidal deviation.

6. Influence of inertia on heat pump behaviour and efficiency

The developed two-mass model approximates a building with a heating system. Both real buildings and real heating systems are diverse. Heating systems can be divided into two categories: radiator systems and underfloor heating systems. Within the two-mass model, the diversity of these systems is represented by the time constant of each system. The time constant is a parameter that describes the inertia of a system. Within this project, we investigate the influence of the heating system's and building's inertia on the heat pump's behaviour and efficiency.

The inertia study consists of six experiments in test point C (outdoor air temperature of 7 °C) with different time constants. With regard to the standard inertia in test point C, three experiments with lower inertia and two with higher inertia were conducted. Table 4 gives an overview of the experiments.

Table 4: Overview of conducted experiments to study the influence of inertia on COP and operating behaviour.

Experiment designation	Inertia heating system (in s)	Inertia building (in s)
Test C	$1 \cdot 1957$	$1 \cdot 209125$
Test C 05x inertia	$0.5 \cdot 1957$	$0.5 \cdot 209125$
Test C 025x inertia	$0.25 \cdot 1957$	$0.25 \cdot 209125$
Test C 0125x inertia	$0.125 \cdot 1957$	$0.125 \cdot 209125$
Test C 2x inertia	$2 \cdot 1957$	$2 \cdot 209125$
Test C 4x inertia	$4 \cdot 1957$	$4 \cdot 209125$

When comparing experiments with different inertia it is essential to adjust the heating curve to guarantee the same temperature level in all experiments. Therefore, several iterations of test point C with different heating curve settings were performed. The final results of the hydraulic temperatures are illustrated in Figure 30 and Figure 31. The average supply temperature differs only between 38.1 °C and 37.5 °C. First, the experiments with reduced inertia are discussed.

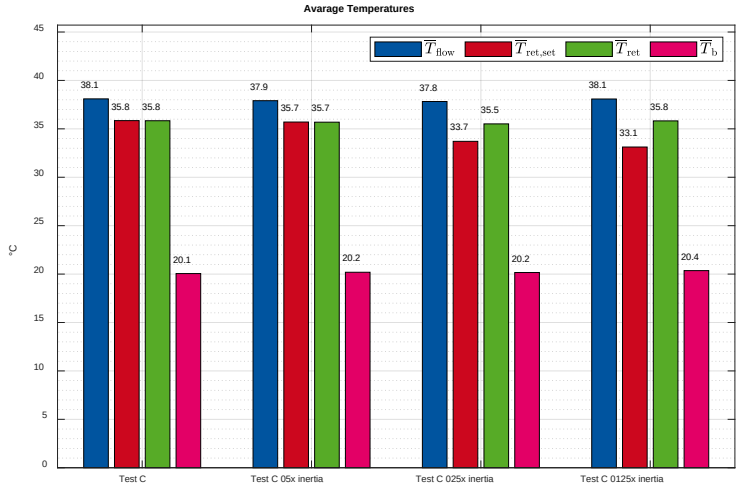

Figure 30: Hydraulic, average temperatures for test point C and corresponding tests with reduced inertia

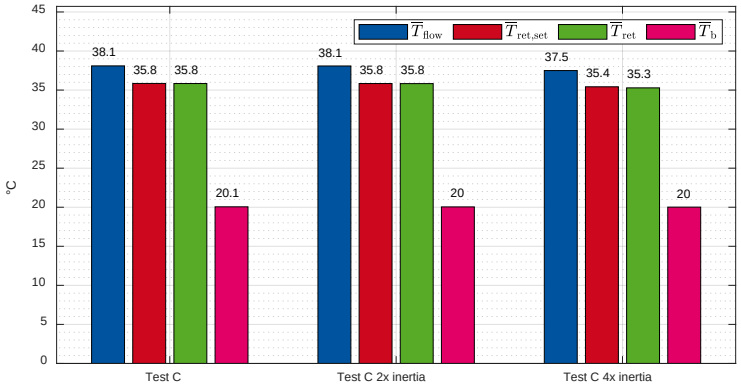

Figure 31: Hydraulic, average temperatures for test point C and corresponding tests with increased inertia

Figure 32 shows the time-dependent data of the supply and return temperature, the heat flows within the two-mass model and the virtual building temperature for the reduced inertia tests. First, it can be observed that the operating behaviour changes with reduced inertia. The lower the inertia, the higher the maximum and the lower the minimum supply temperature. While the 50 % reduced inertia does not affect the cycling periods, the reduction to 25 % and 12.5 % does. The heat pump changes the operating behaviour for 25 % and 12.5 % reduced inertia. A concise cycle follows after two to five reproducible on/off cycles. Furthermore, the virtual building temperature is unstable for the two lowest inertia tests. This behaviour results from the small building mass.

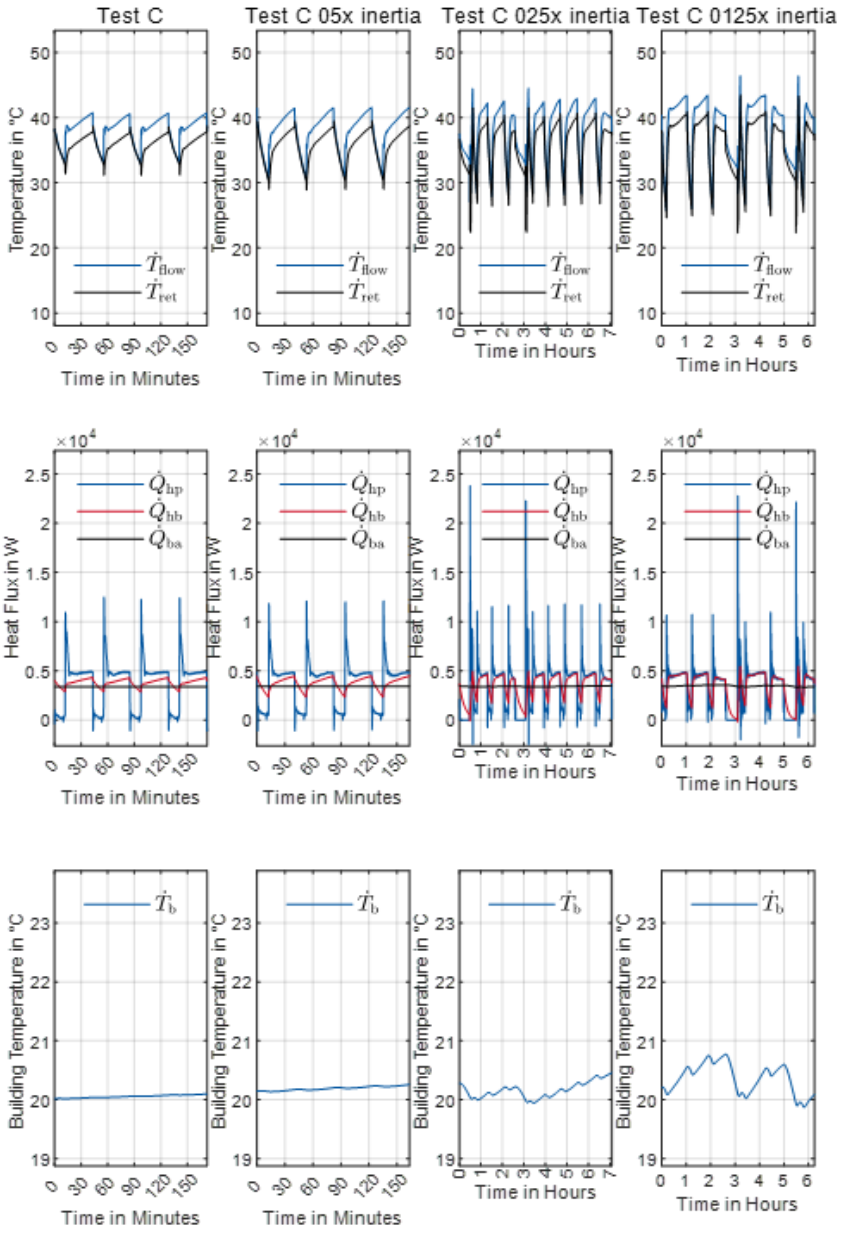

Figure 32: Hydraulic temperatures, two-mass model heat flows and virtual building temperature for test point C and corresponding tests with reduced inertia

Figure 33 shows the hydraulic temperatures, the heat flows within the two-mass model and the virtual building temperature for the experiments with increased inertia. In comparison to reduced inertia, increased inertia directly influences the cycling period. The higher the inertia, the longer the cycling periods. While a complete cycle (on and off period) takes 45 min for typical inertia, it takes 70 min for doubled inertia and 120 min for quadruple inertia. Additionally, the heat pump reacts to the quadruple inertia by adding a short on period before each cycle.

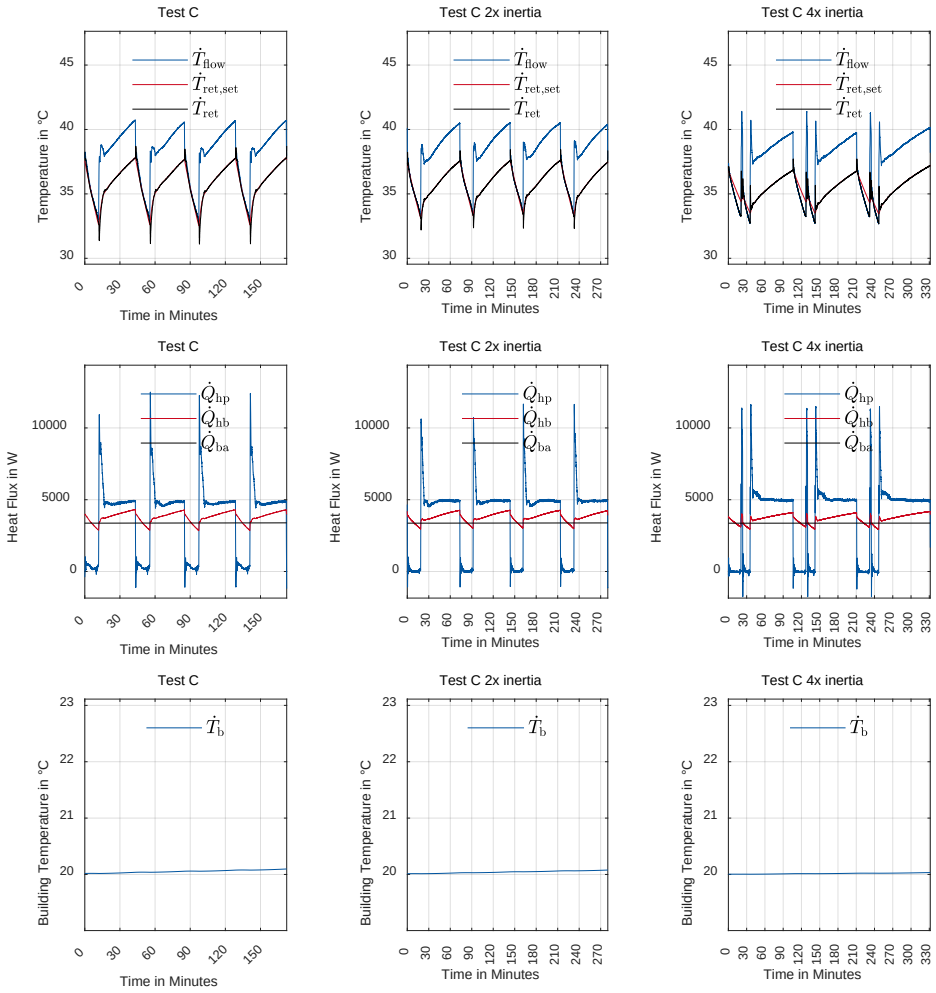

Figure 33: Hydraulic temperatures, two-mass model heat flows and virtual building temperature for test point C and corresponding tests with increased inertia.

Table 5: Measured COP for all conducted experiments with different inertia

Experiment designation	Measured COP
Test C 0125x inertia	3.26
Test C 025x inertia	3.40
Test C 05x inertia	3.55
Test C	3.57
Test C 2x inertia	3.60
Test C 4x inertia	3.66

The results show that inertia affects the heat pump's operating behaviour by changing the cycling periods and the temperature level during on-phases. Therefore, different inertia require different heat curve settings to operate the heat pump at the same average supply temperature

level. To increase reproducibility, standardised tests should be conducted with the same heat pump settings, thus, with the same inertia. Additionally, the inertia affects the overall efficiency of the heat pump system. The COP changes from 3.26 to 3.66 (Table 5). If the experiments with very low inertia (12.5 % and 25 % inertia) are not taken into account, the measured COP are between 3.55 and 3.66. Generally, a clear trend can be obtained: the higher the inertia, the longer the cycle period, and the higher the COP.

Due to the linear appearance of the trend (compare Figure 34), a one-way ANOVA F-test was carried out to assess if COP depends on inertia.

$$COP = b_0 + b_1 \cdot factor + \epsilon$$
$$\epsilon \sim N(0, \sigma^2)$$

Under the assumption of a linear model, the F-test rejects the hypothesis of no-trend with more than 99.9 % certainty.

The Mann-Kendall test further supports the thesis of a real trend. This non-parametric test does not rely on the assumption of a linear model. It only checks for a monotonic increase/decrease by counting the signs of $x_j - x_i$, with i < j for all value pairs:

$$S = \sum_{i-1}^{n-1} \sum_{j=i+1}^{n} sgn(x_j - x_i)$$

The Mann-Kendall test rejects the hypothesis of no trend with 90 % (p = 0.089 < 0.1). Based on the two statistical tests it is unlikely that the measured COPs show no trend.

While identifying a trend becomes more challenging with increased uncertainties in measured values, both tests refrain from assuming any specific conditions regarding uncertainties. They are formulated to be applicable across a spectrum of uncertainties, ranging from small to substantial. Notably, the Mann-Kendall test exhibits resilience against variations in uncertainty. Regardless of the extent to which measured values fluctuate around the true value, the probability of observing four consecutive increasing measurements, in the absence of an underlying trend, remains below 10%. Therefore, this study clearly underlines the need to aligne inertia of different test stands to ensure reproducibility of measurements.

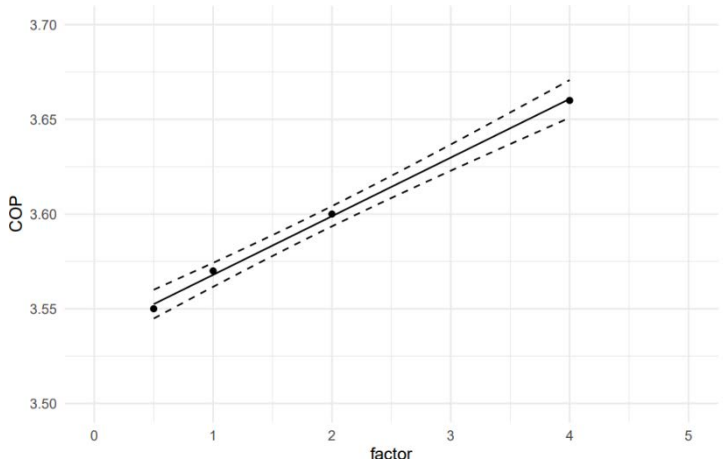

Figure 34: Linear regression and 95% confidence intervals.

7. Transfer of project results

Based on the project results the BAM test guideline on load-based testing of hydronic heat pumps has been fundamentally revised. It includes the two-mass building model to align inertia of different test stands while integrating the heat pump controller into the assessment. The guideline and all publications on the compensation method have been published on a dedicated project website of BAM.[14] It also includes a link to a public BAM Github repository of BAM where the python script developed by RWTH is hosted. The website should make all documents on the compensation method centrally and publicly accessible. The link to the website has been distributed to stakeholders.

In addition, BAM has organised a webinar in April 2023 and present preliminary project results from the PoC to stakeholders, member state representatives and the EU-Commission. The meeting was scheduled before the Commission's Consulation Forum on lot 1 (regulations on central heating appliances covering heat pumps). Initially a physical meeting was organised at the ISH trade fair in Frankfurt am Main in March 2023 which had to be cancelled due to sickness. BAM transferred the project results also to standardisation. BAM is member of CEN/TC 113/WG 8 which works on the compensation method. In March 2023 the PoC results were presented to the working group and a first version of the revised test guideline was shared. In June 2023 an update was provided by BAM. The final report will also be shared with the working group and stakeholders, member state representatives as well as the EU-Commission. BAM is also member of ISO/TC 86/SC 6/TG 13 and transfers the findings from the proof of concept on international level.

[14] https://netzwerke.bam.de/Netzwerke/Navigation/DE/Evpg/EVPG-Waermepumpenpruefung/evpg-waermepumpenpruefung.html

Finally, the project partners are preparing a peer reviewed publication of the project results. Due to resource constrains the publication could not be finalised within the project period and will be submitted in the coming months.

8. Summary and Conclusion

In this PoC on the compensation method the interaction between the heat pump's and the test stand's control is studied. Compared to previous versions of the compensation method, the test bench control includes a building model to emulate the response of a virtual building. On the one hand, the building model is introduced to ensure representative test stand response (inertia) and thus operating behaviour of the heat pump. On the other hand, the model ensures reproducible test results by aligning inertia of different test rigs. With the building model, this is achieved through technology-neutral prescriptions.

In this study, compensation measurements including the building model were performed for the first time. The tests were performed on three different test stands and different test stand deisgns (direct and indirect method) to assess whether the new methodology can be applied on common test rigs. Each lab tested a heat pump from a different manufacturer to extend the range of heat pump controllers. In addition, different controller settings were investigated to prove the applicability of the method for common control strategies (fixed and variable flow; heating curve and indoor temperature control).

First, the feasibility of the method was investigated in the three laboratories. The building model was successfully integrated into the three test bench controls. It has been proven that also test stands optimised for fixed frequency testing according to EN 14511 (especially the indirect test stand of lab 2) can emulate the return temperatures calculated by the building model. In general, the higher dynamics in load-based tests pose higher requirements on the test stand compared to steady-state tests. Nevertheless, good control behaviour of the test rigs could be observed resulting in low deviations of the return temperature from the calculated set point. Only for very high dynamics (load changes) during defrost higher deviations were observed. However, this can be avoided by minor modification of the test rigs to allow also for heating (e.g. adding and electrical heater in the test stand's water loop) depending on the operating mode of the heat pump. Furthermore, flow dependent PID settings will improve controllability at low flow rates during variable flow measurements. The tests revealed that software and hardware modifications necessary to perform compensation measurements can be realised in short time. The related costs are comparably low even if a new mixing station dedicated to compensation measurements would be build. The findings indicate that minor changes in the test setup reveals very high potential to test and asses heat pumps under more realistic boundary conditions which finally is the key for representative labeling.

After successful implementation of the building model in the three test rigs, the second part of the project investigated the operating behavior under various test conditions. All measurements

performed by the three labs showed realistic operating behaviour of the different heat pumps. It has been shown that the test stands handle both constant and variable flows controlled by the heat pump. Moreover, the following observations were made:

- Depending on the heat pump control the heating curve setting might not refer to the average supply temperature over full cycles during on-off operation. Therefore, it might be necessary to adjust the heating curve iteratively. To reduce test time for labs it might be considered to require manufacturers to declare the heating curve settings which can be used as initial start values by the labs. This is not considered an intervention by the manufacturer but further investigations aiming at fully-independet testing could be conducted in the near future.
- PLR C is close to the modulation limit of most compressors. It was found for one heat pump (HP3) that this might lead to switching between operation modes (from on-off cycling to steady-state). However, this observation needs further study. In any case, manufacturers have an incentive to ensure reproducible test results because of market surveillance. By carefully choosing P_{design} PLR C can be moved away from the tipping point, for example. Therefore, the observation is not considered problematic. It should be noted that the measurement just reveals how the unit would operate in the field and does not question the methodology itself.
- The representativeness of test results can also be increased by including the electrical back-up heater in the test since also the controllability of the back-up heater is tested. Lab 1 and lab 2 have proven the feasibility. On the one hand, including the back-up heater in the test may bring additional challenges in terms of repeatability and reproducibility of the measurements, especially if the heat pump controller lacks very good system control. On the other hand, since this is especially true for bad controller designs, better controllability of the back-up heater will be incentivised reducing the overall energy consumption in the field. From a regulatory point of view testing with active back-up heater was challenged because for some products the heat pump and the back-up heater are placed separately on the market. To allow for testing of those products a virtual back-up heater can be implemented in the test which automatically compensates any lack in heating capacity.[15] In the ongoing round robin test, both options will be assessed more deeply to develop a solid proposal that ensures reproducibility while aiming at representative testing conditions for the benefit of users.
- Tests with active indoor temperature control demonstrate that the calculated building temperature can be used to test also heat pumps with controllers processing the indoor air room temperature. For this proof of concept the building temperature was emulated manually, however, automated climate boxes are state of the art and can be easily implemented in the test rig setup. The tests revealed that the building temperature

[15] This concept has already successfully been tested in preparation of the ongoing round robin test. For realistic operation of the virtual back-up heater its heating power was limited to the declared maximum power of the real back-up heater. In the round robin test both approaches (real vs. virtual back-up heater) are assessed.

might not be a good approximation for the room air temperature. Therefore, the heat transfer between the heating system (mass H) and the building walls must be reviewed to ensure consistency between supply and room air temperature changes. However, the effort for the potential extension of the two-mass model is manageable in rather short time and can be foreseen for future studies since heat pumps without a heating curve function relying on outdoor temperature are not common.

- COP and $SCOP_{on}$ values derived from compensation measurements with electrical back-up heater and standard measurements according to EN 14511 are compared for HP1 and HP2. Similar to previous work significant deviations are observed at low part load conditions (PLR D) due to more realistic testing according to the compensation method with active control. Including the back-up heater (and its control) in the test and capturing at least one defrost cycle for conditions where icing coccurs yields lower more realistic test results and incentivises efficient defrost strategies. The lower COPs translate in decreased $SCOP_{on}$ values for the compensation method.[16] However, this difference can be smaller (HP2) or larger (HP1) underlining the importance for more representative testing incentivising better energy performance of heat pumps.

In the third project part, a sensitivity analysis was performed to assess appropriate permissible deviations on the return temperature required by a future standard. The conducted study indicates that permissible deviations on the return temperature in the range of 0.5-1 K are low enough to ensure an acceptable level of repeatability and reproducibility of COP. Higher deviations occur during events with high dynamics, such as defrost or compressor start during on-off operation. For those events higher permissible deviations are unlikely to affect the operating behaviour of the heat pump. Therefore, in the revised guideline permissible deviations of +2/-5 K have been taken over from EN 14511 for defrost and no permissible deviations are set for a limited time after compressor start. The planned round robin test (38943/01) will provide further information how tight the permissible deviations can/must be set.

Finally, it has been shown that inertia must be aligned between different test stands. Inertia changes the operating behaviour of the heat pump and, thus, the COP. Eventhough the observed COP trend is rather small, if very low inertias are excluded, it should be considered that (a) any difference in COP reduces reproducibility, (b) test conditions must be aligned to ensure comparability (aligne operating behaviour) and (c) the COP difference might be dependent on the controller and/or the refrigerant circuit and only a single unit has been tested. With regard to the last point, it.has been proven that the operating behaviour, in particular, the temperature level during on phases of the compressor changes with inertia and different refrigerant circuits (refrigerants) may respond more sensitive to those changes than others. Therefore, higher differences in COP might be observed for different heat pumps.

[16] In general, results under PLRD have less impact on the SCOP because of the lower weighting in the bin calculation. In contrast, the COP at PLRB has a much stronger impact on the SCOP.

In summary, the measurements confirmed the expected interaction between the test 'stands' and heat 'pumps' controls. Realistic operating behaviour was observed and confirmed in three labs with three heat pumps. In addition, the methodology can be implemented on existing test rigs in rather short time and at low cost while already reaching a sufficient level of control on the return temperature. Hence, the PoC has been successful and the validation phase is started with a follow-up project (38943/01) .

9. Acknowledgement

The authors are gratefull for the support and funding by the Deutsche Bundesstiftung Umwelt. The partners also thank the manufacturers of the heat pumps for providing the units for the testing. We also greatly appreciate the excellent collaboration with Andreas Zottl (AIT) and Ralf Noack (ILK) and we thank the whole team of the three labs for carrying out the measurements.

References

1. Simo, A., C. Palkowski, and A. Wachau, *Proposal for the revision of the harmonised test standard EN 14825:2016*. 2019, Federal Institute for Materials Research and Testing (BAM).
2. ; Available from: https://netzwerke.bam.de/Netzwerke/Navigation/EN/Ecodesign/Nape/nape.html.
3. Wachau, A., D. Mock, and P. Minelli, *BAM technical report on load-based testing of hydronic heat pumps - compensation method*. 2023, Bundesanstalt für Materialforschung und -prüfung (BAM).
4. Göbel, S., et al., *How to measure and evaluate refrigerant cycles – in a representative, reproducible manner? An experimental case study for water-to-water heat pumps*, in *19th International Refrigeration and Air Conditioning Conference at Purdue*. 2022: Purdue University (USA).
5. Göbel, S., et al., *How to calibrate heat pump test stands for load-based testing – towards technology-neutral prescriptions.* Energy Proceedings 2022.
6. Mehrfeld, P., *Evaluation of heat pump systems under dynamic operating conditions; 1. Auflage*, in *E.ON Energy Research Center ; EBC, Energy efficient buildings and indoor climate*. 2022, RWTH Aachen University: Aachen. p. 1 Online-Ressource : Illustrationen, Diagramme.
7. CLASP, *Better heat pumps from better testing*. 2023, CLASP.